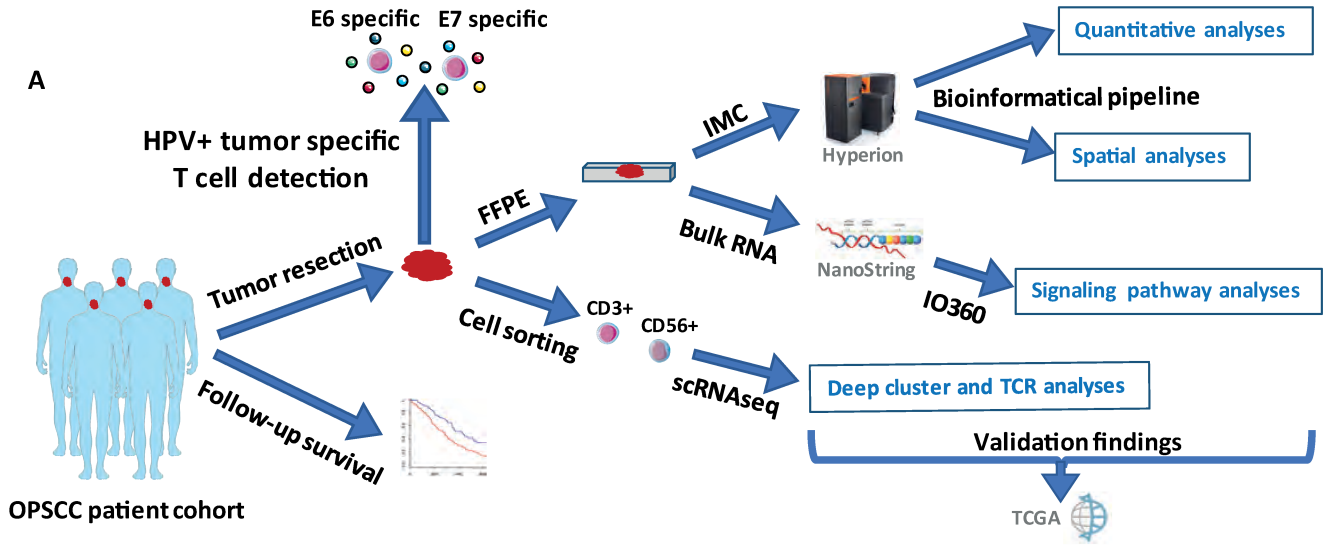

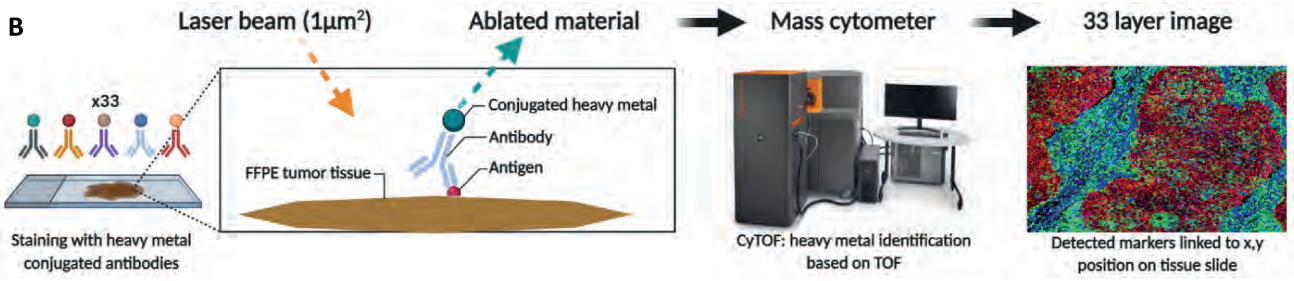

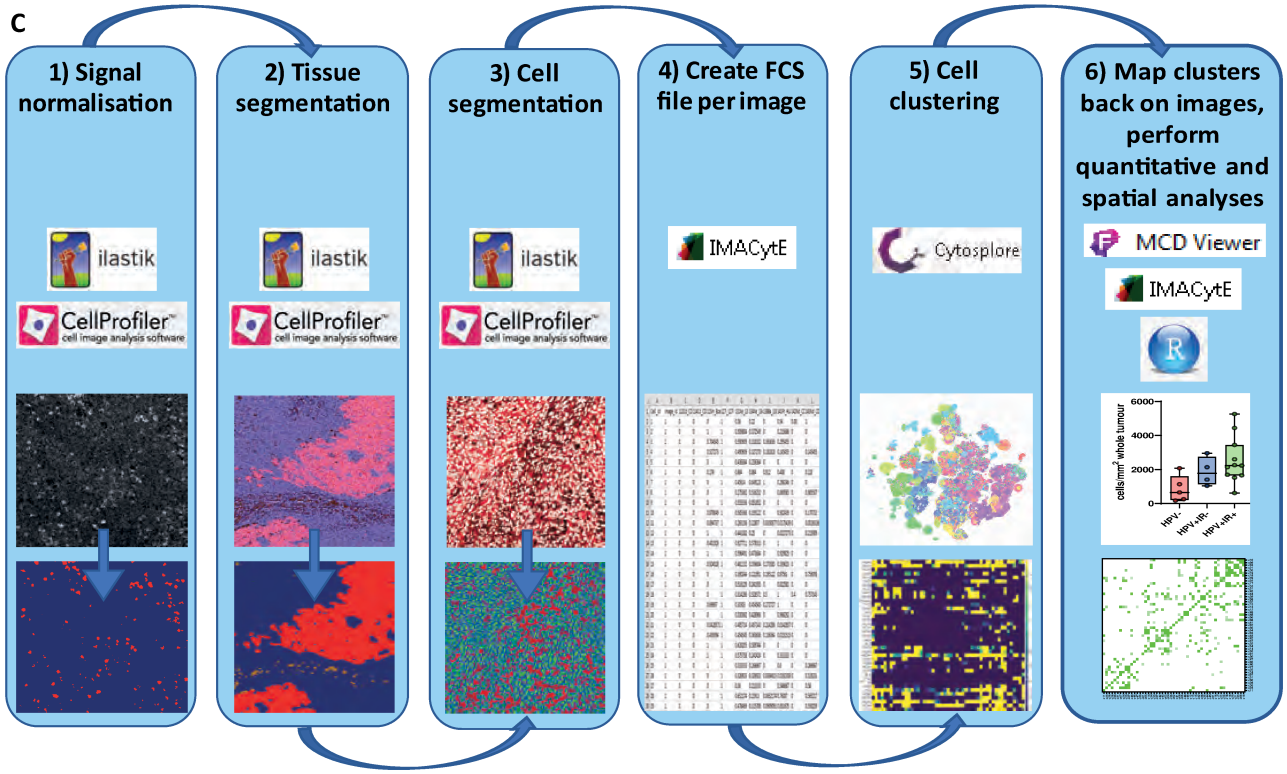

D

	OPSCC total (n=20)	HPV- (n=5)	HPV+IR- (n=4)	HPV+IR+ (n=11)
Immune cells	274,775	45,139	46,204	183,432
Tumor cells	142,868	38,015	37,247	67,606
Stromal cells	46,907	15,149	11,045	20,713
Total cells	464,550	98,303	94,496	271,751

Supplemental Figure 1. Bioinformatical pipeline imaging mass cytometry data analyses.
A) Overview of the multi-dimensional study workflow yielding comprehensive high-dimensional information of the immune landscape of Oropharyngeal Squamous Cell Carcinoma (OPSCC). FFPE=formalin-fixed paraffin-embedded; IMC=imaging mass cytometry; scRNAseq=single cell RNA sequencing; TCR=T cell receptor; TCGA=the cancer genome atlas. B) Visualization of the imaging mass cytometry staining and image acquisition workflow. Image created with BioRender. C) All analytical steps performed to process the imaging mass cytometry data, including the programs used to perform that analytical step, and visualization of the stepwise image processing. D) Counts of cells analyzed by imaging mass cytometry in the total OPSCC cohort and per subgroup, of immune cells, tumor cells, stromal cells and the total of all cells analyzed.

Supplemental Table 1. OPSCC patient characteristics.

Patient ID *	Sex	Age **	Tumor location	pTNM stage	HPV16 status	IR status ***	Received treatment	Analysis techniques
H62	M	61	Tongue base	4a-2c-0	+	-	RT	NanoString
H68	F	64	Tonsil	3-2b-0	+	+	RT	Hyperion, scRNAseq, NanoString, Luminex
H71	F	62	Tongue base	2-2c-0	+	+	RT	Hyperion, NanoString
H72	M	58	Tongue base	2-0-0	-	-	RT	Hyperion, NanoString
H74	F	65	Tonsil	4a-0-0	-	-	none	Hyperion, NanoString
H77	M	48	Tonsillar fossa	1-2a-0	+	+	S+RT	Hyperion, NanoString
H78	M	54	Tonsillar fossa	2-0-0	-	-	RT	NanoString
H93	M	57	Tongue base	1-2b-0	+	+	S+RT	Hyperion, NanoString
H95	M	59	Tongue base	2-1-0	+	+	RT	NanoString
H125	M	64	Posterior wall	3-0-0	-	-	CT+RT	NanoString
H136	V	47	Tonsil	2-2b-0	+	+	CT+RT	Hyperion, NanoString, Luminex
H138	M	74	Tongue base	2-0-0	+	+	RT	Hyperion, Luminex
H141	M	67	Tongue base	2-2b-0	+	+	CT+RT	Hyperion, scRNAseq, NanoString
H143	V	74	Tonsil	1-2a-0	-	-	RT	Hyperion, scRNAseq, NanoString
H148	V	64	Tonsil	2-2b-0	+	+	S+RT	Luminex
H149	V	47	Tonsil	2-2a-0	+	-	S+RT	Hyperion, scRNAseq, NanoString, Luminex
H150	M	59	Tonsil	2-2a-0	+	-	S+RT	Luminex
H159	V	67	Tonsil	4a-2c-0	+	+	CT+RT	Luminex
H160	M	69	Tongue base	2-2b-0	+	+	CT+RT	Hyperion, scRNAseq, NanoString, Luminex
H161	V	65	Tongue base	2-2b-0	+	+	S+RT	Luminex
H176	M	52	Tongue base	3-0-0	+	+	CT+RT	Hyperion, scRNAseq, NanoString
H180	M	59	Tonsil	2-2a-0	+	+	RT	Luminex
H182	M	66	Tongue base	4-3-0	+	-	CT	Hyperion, scRNAseq, NanoString
H185	M	58	Tongue base	2-0-0	+	+	RT	Hyperion, scRNAseq, NanoString
H187	V	67	Pallatum mole	2-0-0	-	-	RT	NanoString
H188	V	56	Tonsil	3-0-0	+	+	CT+RT	Hyperion, scRNAseq, NanoString, Luminex
H191	M	39	Tonsil	2-2b-0	+	-	RT	Luminex
H197	V	63	Tonsil	4b-0-0	-	-	CT+RT+CX	Hyperion, scRNAseq, NanoString
H205	M	56	Tonsil	4a-2b-1	-	-	RT	Hyperion, scRNAseq, NanoString
H208	M	60	Tongue base	4-2a-0	+	-	CT+RT	Hyperion, scRNAseq, NanoString, Luminex
H211	M	62	Tongue base	3-2b-0	+	-	CT+RT	Hyperion, scRNAseq, NanoString, Luminex

* 'H' indicates OPSCC patients included in the P07-112 head and neck cancer study

** Age at diagnosis and sampling of tumor tissue pre-therapy

*** Immune response (IR) status was determined by analyzing cultured tumor infiltrating lymphocytes for the presence of HPV16-specific T cells using a [3H]-thymidine-based proliferation assay and antigen-specific cytokine production assay

CT: chemotherapy; CX: cetuximab; F: female; M: male; pTNM: pathological Tumor, lymph Nodes, Metastasis; RT: radiotherapy; S: surgical resection

Supplemental Table 2. Definition of NanoString nSolver cell types.

Cell type	Gene	Cell type	Gene	Cell type	Gene
CD45	*PTPRC*	CD8	*CD8A*	Macrophage	*CD163*
T cells	*CD3D*		*CD8B*		*CD68*
	CD3E	Th1	*TBX21*		*CD84*
	CD3G	Treg	*FOXP3*		*MS4A4A*
	CD6	Exhausted CD8	*CD244*	Neutrophils	*CEACAM3*
	SH2D1A		*EOMES*		*CSF3R*
	TRAT1		*LAG3*		*FCAR*
B cells	*BLK*		*PTGER4*		*FPR1*
	CD19	Cytotoxic cell	*CTSW*		*S100A12*
	FCRL2		*GNLY*		*SIGLEC5*
	MS4A1		*GZMA*	NK cells	*NCR1*
	PNOC		*GZMB*	NK CD56dim	*IL21R*
	SPIB		*GZMH*		*KIR2DL3*
	TCL1A		*KLRB1*		*KIR3DL1*
	TNFRSF17		*KLRD1*		*KIR3DL2*
DC	*CCL13*		*KLRK1*	Mast cells	*CPA3*
	CD209		*NKG7*		*HDC*
	HSD11B1		*PRF1*		*MS4A2*

Cell types as automatically defined by the expression of the indicated genes by NanoString nSolver software.

Supplemental Table 3. Imaging mass cytometry 33-marker panel.

Marker	Antibody clone	Conjugated heavy metal	Antibody dilution	Incubation conditions
HLA-DR	TAL1B5	^{141}Pr	1:100	5 hours at room temperature
CD11b	D6X1N	^{144}Nd	1:100	5 hours at room temperature
CD4	EPR6855	^{145}Nd	1:50	5 hours at room temperature
CD8	D8A8Y	^{146}Nd	1:50	5 hours at room temperature
CD73	D7F9A	^{148}Nd	1:100	5 hours at room temperature
TGFβ	TB21	^{149}Sm	1:100	5 hours at room temperature
PD-L1	E1L3N(R)	^{156}Gd	1:100	5 hours at room temperature
FoxP3	D608R	^{159}Tb	1:100	5 hours at room temperature
IDO	D5J4E(TM)	^{162}Dy	1:50	5 hours at room temperature
CD204	J5HTR3	^{164}Dy	1:100	5 hours at room temperature
CD45ro	UCHL1	^{165}Ho	1:50	5 hours at room temperature
CD38	EPR4106	^{169}Tm	1:50	5 hours at room temperature
CD163	EPR14643-36	^{173}Yb	1:100	5 hours at room temperature
CD7	EPR4242	^{174}Yb	1:50	5 hours at room temperature
P16	D3W8G	^{175}Lu	1:100	5 hours at room temperature
Vimentin	D21H3	^{194}Pt	1:100	5 hours at room temperature
β-catenin	D10A8	^{115}In	1:100	overnight at 4 degrees Celsius
CD20	H1	^{142}Nd	1:100	overnight at 4 degrees Celsius
CD68	D4B9C	^{143}Nd	1:100	overnight at 4 degrees Celsius
CD31	89C2	^{147}Sm	1:100	overnight at 4 degrees Celsius
CD57	HNK-1/Leu-7	^{151}Eu	1:100	overnight at 4 degrees Celsius
Ki67	8D5	^{152}Sm	1:100	overnight at 4 degrees Celsius
CD3	D7AGE(TM)	^{153}Eu	1:50	overnight at 4 degrees Celsius
VISTA	D1L2G(TM)	^{158}Gd	1:50	overnight at 4 degrees Celsius
ICOS	D1K2T(TM)	^{161}Dy	1:50	overnight at 4 degrees Celsius
CD14	D7A2T	^{163}Dy	1:100	overnight at 4 degrees Celsius
D2-40	D2-40	^{166}Er	1:100	overnight at 4 degrees Celsius
CD56	EPR2566	^{167}Er	1:100	overnight at 4 degrees Celsius
CD103	EPR4166(2)	^{168}Er	1:100	overnight at 4 degrees Celsius
CD15	BRA-4F1	^{171}Yb	1:100	overnight at 4 degrees Celsius
Cleaved-caspase	ASP175	^{172}Yb	1:100	overnight at 4 degrees Celsius
CD11c	EP1347Y	^{176}Yb	1:100	overnight at 4 degrees Celsius
Keratin	C11 and AE1/AE3	^{198}Pt	1:50	overnight at 4 degrees Celsius

Supplemental Table 4A. Differentially expressed genes (DEGs) between HPV16^{+}IR^{+} and HPV16^{+}IR^{-} OPSCC patients.

DEG	Log2 fold change	SD	P-value	Method	Corrected P-value
CCL20	-3.67	0.647	2.20E-05	Lm.nb	0.0124
BMP2	-2.68	0.512	5.60E-05	Lm.nb	0.0124
BLK	5.85	1.13	6.35E-05	Lm.nb	0.0124
HLA-DRB1	3.55	0.705	8.73E-05	Lm.nb	0.0124
CXCL3	-3.25	0.652	9.56E-05	Lm.nb	0.0124
LTB	5.22	1.06	0.00011	Lm.nb	0.0124
PFKFB3	-1.69	0.347	0.000123	Lm.nb	0.0124
CXCL12	4.59	0.98	0.000186	Lm.nb	0.0164
CCL19	4.1	0.943	0.000386	Lm.nb	0.028
CSF2	-4.26	0.984	4.00E-04	Lm.nb	0.028
TNFSF13	4.08	0.962	0.000489	Lm.nb	0.028
NLRC5	1.84	0.439	0.000539	Lm.nb	0.028
HLA-DQA2	-6.12	1.45	0.000586	Wald	0.028
HSD11B1	3.21	0.771	0.000639	Wald	0.028
TNFRSF18	3.71	0.9	0.00064	Lm.nb	0.028
PIK3CD	3.03	0.745	0.000721	Lm.nb	0.028
HLA-A	2.87	0.706	0.000737	Lm.nb	0.028
TREM1	-2.56	0.633	0.000762	Lm.nb	0.028
INHBA	-3.93	0.98	0.000819	Lm.nb	0.028
IL1B	-3.16	0.791	0.000834	Lm.nb	0.028
LILRB4	3	0.751	0.000837	Lm.nb	0.028
HRAS	3.66	0.921	0.000891	Lm.nb	0.028
KLRD1	3.38	0.845	0.000913	Wald	0.028
CXCL8	-3.65	0.928	0.000968	Lm.nb	0.0285
IL11	-3.43	0.885	0.00112	Lm.nb	0.0308
IKBKB	2.79	0.724	0.00115	Lm.nb	0.0308
HLA-F	3.62	0.946	0.00123	Lm.nb	0.0308
CD79A	3.74	0.985	0.00132	Lm.nb	0.0308
TNFSF9	3.57	0.931	0.00132	Wald	0.0308
APOL6	2.87	0.755	0.00132	Lm.nb	0.0308
CD58	2.59	0.684	0.00135	Lm.nb	0.0308
PNOC	2.84	0.75	0.00148	Wald	0.0325
IRF5	1.55	0.417	0.00156	Lm.nb	0.0325
NEIL1	2.11	0.569	0.00159	Lm.nb	0.0325
IRF4	2.97	0.801	0.00161	Lm.nb	0.0325
IL6R	2.16	0.586	0.00167	Lm.nb	0.0326
LYZ	1.79	0.487	0.00171	Lm.nb	0.0326
CD6	2.59	0.709	0.0018	Lm.nb	0.0329
PGPEP1	2.61	0.715	0.00182	Lm.nb	0.0329
GZMM	2.41	0.656	0.0019	Wald	0.0336
PSMB10	2.03	0.577	0.00246	Lm.nb	0.0424
CTSW	2.79	0.798	0.00258	Lm.nb	0.0434
TGFB1	2.9	0.845	0.00295	Lm.nb	0.0474

Supplemental Table 4B. Differentially expressed genes (DEGs) between HPV16^{+}IR^{-} and HPV^{-} OPSCC patients.

DEG	Log2 fold change	SD	P-value	Method	Corrected P-value
CCL20	3.25	0.628	6.43E-05	lm.nb	0.0454

Supplemental Table 4C. Differentially expressed genes (DEGs) between HPV16^{+}IR^{+} and HPV^{-} OPSCC patients.

DEG	Log2 fold change	SD	P-value	Method	Corrected P-value
CXCL12	5.74	0.912	6.21E-06	lm.nb	0.00259
LTB	6.04	0.986	8.60E-06	lm.nb	0.00259
KLRD1	4.19	0.743	2.92E-05	Wald	0.00259
BBC3	2.71	0.493	3.22E-05	lm.nb	0.00259
BLK	5.75	1.05	3.40E-05	lm.nb	0.00259
PIK3CD	3.73	0.693	4.06E-05	lm.nb	0.00259
TNFSF13	4.8	0.895	4.28E-05	lm.nb	0.00259
IKBKB	3.61	0.673	4.29E-05	lm.nb	0.00259
UBA7	4.44	0.831	4.42E-05	lm.nb	0.00259
HRAS	4.57	0.856	4.49E-05	lm.nb	0.00259
APOL6	3.73	0.702	4.77E-05	lm.nb	0.00259
HLA-F	4.65	0.88	5.06E-05	lm.nb	0.00259
C5	3.3	0.628	5.40E-05	lm.nb	0.00259
DNMT1	3.69	0.703	5.43E-05	lm.nb	0.00259
DDB2	3.49	0.666	5.50E-05	lm.nb	0.00259
ICAM5	5.15	0.988	5.89E-05	lm.nb	0.0026
GNLY	3.58	0.704	7.82E-05	lm.nb	0.00325
GZMB	3.65	0.712	8.35E-05	Wald	0.00327
POLD1	1.78	0.357	9.52E-05	lm.nb	0.00329
LILRB4	3.48	0.698	9.58E-05	lm.nb	0.00329
VHL	2.91	0.586	9.77E-05	lm.nb	0.00329
CD58	3.13	0.637	0.000113	lm.nb	0.00362
GLS	4.02	0.831	0.000134	lm.nb	0.00406
CCL19	4.22	0.877	0.000138	lm.nb	0.00406
DLL4	3.03	0.636	0.000157	lm.nb	0.00426
TGFB1	3.73	0.786	0.00016	lm.nb	0.00426
PGPEP1	3.16	0.666	0.000163	lm.nb	0.00426
MSH6	3.56	0.757	0.000177	lm.nb	0.00446
CCND1	-2.87	0.612	0.000186	lm.nb	0.00453
PIK3R2	3.52	0.758	0.000203	lm.nb	0.00477
CTLA4	3.04	0.659	0.000212	lm.nb	0.00477
CSF1	2.87	0.623	0.000216	lm.nb	0.00477
NLRP3	4.44	0.97	0.000235	lm.nb	0.00503
CD7	3.14	0.691	0.000252	lm.nb	0.00516
CD80	2.73	0.604	0.000261	lm.nb	0.00516
IRF7	1.43	0.316	0.000263	lm.nb	0.00516
HSD11B1	3.23	0.707	0.000277	Wald	0.00529
FANCA	2.29	0.513	0.000301	lm.nb	0.00559

DEG	Log2 fold change	SD	P-value	Method	Corrected P-value
EZH2	1.02	0.228	0.000309	lm.nb	0.0056
IRF1	2.44	0.549	0.000318	lm.nb	0.0056
CSF2RB	2.75	0.622	0.00033	lm.nb	0.00568
JAK2	2.41	0.55	0.000361	lm.nb	0.00585
HLA-DRB1	2.87	0.656	0.000364	lm.nb	0.00585
NLRC5	1.78	0.408	0.000377	lm.nb	0.00585
NOTCH1	2.32	0.531	0.000377	lm.nb	0.00585
TNFRSF25	2.29	0.526	0.000389	lm.nb	0.00585
CHUK	2.66	0.611	0.000393	lm.nb	0.00585
AXL	3.3	0.761	0.000397	lm.nb	0.00585
JAG2	3.41	0.782	0.000427	Wald	0.00615
MB21D1	0.921	0.215	0.000455	lm.nb	0.00632
CCL18	2.68	0.626	0.000456	lm.nb	0.00632
PPARGC1B	2.1	0.494	0.000472	lm.nb	0.00641
ULBP2	-2.19	0.518	0.000505	lm.nb	0.00654
TMEM140	2.53	0.599	0.000507	lm.nb	0.00654
CYBB	2.78	0.657	0.000509	lm.nb	0.00654
PSMB10	2.25	0.537	0.000555	lm.nb	0.00689
LGALS9	2.78	0.664	0.000557	lm.nb	0.00689
NCR1	2.86	0.682	0.000616	Wald	0.00729
CD68	2.7	0.653	0.000617	lm.nb	0.00729
TNFSF9	3.65	0.873	0.000622	Wald	0.00729
TNFRSF18	3.46	0.837	0.000629	lm.nb	0.00729
RAD51C	2.42	0.591	0.000687	lm.nb	0.00782
CD79A	3.74	0.916	0.000707	lm.nb	0.00792
SIGLEC1	2.65	0.651	0.00073	lm.nb	0.00805
CTSW	3.01	0.743	0.000747	lm.nb	0.00811
PVRIG	2.82	0.699	0.000776	lm.nb	0.0082
MLH1	1.72	0.427	0.000791	lm.nb	0.0082
TIE1	2.82	0.7	0.000798	lm.nb	0.0082
BRD3	2.56	0.638	0.000801	lm.nb	0.0082
MTOR	1.32	0.333	0.000892	lm.nb	0.00885
CD6	2.62	0.659	0.000898	lm.nb	0.00885
TYMS	2.51	0.632	0.000902	lm.nb	0.00885
MELK	1.17	0.295	0.000918	lm.nb	0.00887
IL6R	2.15	0.545	0.00093	lm.nb	0.00887
NFAM1	2.24	0.564	0.000978	Wald	0.00911
TAP2	1.62	0.413	0.00098	lm.nb	0.00911
CD74	2.57	0.656	0.00102	lm.nb	0.00936
JAK3	2.42	0.622	0.00106	lm.nb	0.00958
ZAP70	3.07	0.789	0.00107	lm.nb	0.00958
RELA	2.53	0.652	0.0011	lm.nb	0.0097
NFKB2	2.37	0.612	0.00112	lm.nb	0.00973
BAX	1.24	0.322	0.00115	lm.nb	0.00991
CDK2	1.5	0.393	0.00127	lm.nb	0.0107
TNFRSF1B	2.14	0.563	0.00132	lm.nb	0.0108
IRF3	1.18	0.312	0.00136	lm.nb	0.0108
ITGAL	2.82	0.745	0.00136	lm.nb	0.0108
STAT2	1.13	0.298	0.00137	lm.nb	0.0108
HLA-C	2.67	0.708	0.00138	lm.nb	0.0108

DEG	Log2 fold change	SD	P-value	Method	Corrected P-value
HLA-DMA	2.4	0.637	0.00139	lm.nb	0.0108
HELLS	1.45	0.385	0.0014	lm.nb	0.0108
SBNO2	1.25	0.331	0.0014	lm.nb	0.0108
IRF4	2.78	0.745	0.00153	lm.nb	0.0113
FUT4	2.68	0.72	0.00153	lm.nb	0.0113
CD3D	2.84	0.762	0.00156	lm.nb	0.0113
DUSP5	1.52	0.409	0.00156	lm.nb	0.0113
IKBKG	2.1	0.563	0.00156	lm.nb	0.0113
TREM1	-2.18	0.59	0.00165	lm.nb	0.0118
CD8A	3.13	0.846	0.00166	lm.nb	0.0118
CCL4	1.85	0.503	0.00169	lm.nb	0.0119
TNFSF12	1.91	0.519	0.00175	lm.nb	0.0122
BAD	2.19	0.597	0.00176	lm.nb	0.0122
ITGB2	1.69	0.462	0.00178	lm.nb	0.0122
TRAF1	2.35	0.644	0.00181	lm.nb	0.0122
VSIR	1.87	0.511	0.00181	lm.nb	0.0122
NECTIN2	1.86	0.512	0.00187	lm.nb	0.0125
CX3CL1	1.66	0.462	0.00204	lm.nb	0.0135
TNFRSF14	1.68	0.466	0.00206	lm.nb	0.0135
CD47	1.6	0.445	0.00213	lm.nb	0.0138
CCL5	2.36	0.667	0.00232	lm.nb	0.0149
APOE	2.29	0.653	0.00249	lm.nb	0.0159
TAPBPL	1.38	0.394	0.00253	lm.nb	0.0159
PNOC	2.49	0.707	0.00266	Wald	0.0166
PDGFRB	2.6	0.748	0.00268	lm.nb	0.0166
CXCL9	2.55	0.735	0.00273	lm.nb	0.0168
TMEM173	1.74	0.502	0.00276	lm.nb	0.0168
CD45RO	1.92	0.555	0.0028	lm.nb	0.0169
PTGER4	1.66	0.482	0.00288	lm.nb	0.0172
C1QB	1.82	0.527	0.0029	lm.nb	0.0172
IFNGR2	1.55	0.453	0.00306	lm.nb	0.018
TREM2	2.02	0.592	0.00313	lm.nb	0.0183
LAG3	2.1	0.618	0.00324	lm.nb	0.0188
CEBPB	1.83	0.543	0.00347	lm.nb	0.0199
TGFB3	2.78	0.83	0.00356	lm.nb	0.0203
DLL1	2.02	0.604	0.00368	lm.nb	0.0208
CD3E	2.36	0.709	0.0037	lm.nb	0.0208
TLR7	2.25	0.671	0.00374	Wald	0.0208
IL2RA	1.78	0.535	0.00376	lm.nb	0.0208
HLA-E	1.25	0.376	0.00384	lm.nb	0.0209
GLUD1	1.63	0.491	0.00384	lm.nb	0.0209
EGFR	-1.67	0.505	0.00394	lm.nb	0.0211
CCND3	1.73	0.525	0.00408	lm.nb	0.0214
MMP9	2.72	0.828	0.00412	lm.nb	0.0214
BRD4	1.02	0.311	0.00416	lm.nb	0.0214
MAP3K7	1.55	0.473	0.00421	lm.nb	0.0214
BCAT1	-1.7	0.52	0.00422	lm.nb	0.0214
ITGAX	1.75	0.536	0.00422	lm.nb	0.0214
TAPBP	1.6	0.49	0.00426	lm.nb	0.0214
ITGA4	1.79	0.548	0.00428	lm.nb	0.0214

DEG	Log2 fold change	SD	P-value	Method	Corrected P-value
HLA-A	2.14	0.657	0.00432	lm.nb	0.0215
BCL2L1	1.26	0.388	0.00438	lm.nb	0.0216
RSAD2	2.04	0.632	0.00461	lm.nb	0.0225
IFIH1	1.11	0.343	0.00462	lm.nb	0.0225
BRIP1	1.3	0.404	0.00475	lm.nb	0.023
IFI35	1.69	0.529	0.00503	lm.nb	0.0241
HLA-B	2.02	0.632	0.00505	lm.nb	0.0241
MYD88	0.857	0.269	0.00514	lm.nb	0.0243
GBP2	1.61	0.507	0.00519	lm.nb	0.0244
HERC6	1.8	0.57	0.00542	lm.nb	0.0253
IRF5	1.22	0.387	0.00555	lm.nb	0.0257
MFNG	1.56	0.496	0.00557	lm.nb	0.0257
ICAM3	1.31	0.42	0.00588	lm.nb	0.027
OAS3	1.03	0.329	0.00592	lm.nb	0.027
TNF	1.78	0.571	0.00597	lm.nb	0.027
OAS1	1.03	0.332	0.00601	lm.nb	0.027
MAGEA1	-2.29	0.732	0.00617	Wald	0.0276
PSMB9	1.72	0.556	0.00627	lm.nb	0.0276
VEGFA	1.8	0.582	0.00627	lm.nb	0.0276
CXCL10	2.06	0.668	0.0063	lm.nb	0.0276
APC	1.45	0.472	0.00647	lm.nb	0.0282
BMP2	-1.47	0.477	0.00654	lm.nb	0.0283
DUSP2	1.59	0.52	0.0067	lm.nb	0.0288
IRF9	1.08	0.353	0.00682	lm.nb	0.0292
GBP1	1.41	0.463	0.00697	lm.nb	0.0296
CDKN2A	2.81	0.935	0.00756	lm.nb	0.032
NKG7	2.18	0.726	0.00765	lm.nb	0.0322
OAS2	1.26	0.422	0.00794	lm.nb	0.0329
MARCO	2.47	0.823	0.00797	Wald	0.0329
BRCA2	1.11	0.373	0.00798	lm.nb	0.0329
IFITM1	1.2	0.407	0.00874	lm.nb	0.0359
CXCL6	-2.82	0.964	0.00904	lm.nb	0.0368
CD69	1.37	0.471	0.00919	lm.nb	0.0368
ICAM1	1.02	0.351	0.0092	lm.nb	0.0368
GIMAP4	1.37	0.47	0.00921	lm.nb	0.0368
PARP4	1.14	0.391	0.00925	lm.nb	0.0368
SNAI1	1.74	0.597	0.00929	lm.nb	0.0368
CASP9	1.12	0.386	0.00941	lm.nb	0.0371
CD3G	2.14	0.738	0.00952	lm.nb	0.0371
GPSM3	1.38	0.476	0.0096	lm.nb	0.0371
P4HA2	-3.58	1.24	0.00963	loglinear	0.0371
SGK1	1.58	0.547	0.00974	lm.nb	0.0371
MXI1	1.81	0.626	0.00975	lm.nb	0.0371
FYN	1.16	0.404	0.00993	lm.nb	0.0375
CD4	1.44	0.503	0.0102	lm.nb	0.0383
FAP	-1.33	0.463	0.0104	lm.nb	0.0385
MYC	1.23	0.433	0.0105	lm.nb	0.0389
C1QA	1.3	0.458	0.0106	lm.nb	0.0389
ITGAM	1.61	0.566	0.0106	lm.nb	0.0389
PALMD	2.11	0.744	0.0109	lm.nb	0.0397

DEG	Log2 fold change	SD	P-value	Method	Corrected P-value
IL2RB	1.59	0.561	0.0111	lm.nb	0.0402
IL11	-2.33	0.825	0.0112	lm.nb	0.0402
SH2D1A	2.22	0.787	0.0113	lm.nb	0.0404
BCL2	1.81	0.643	0.0113	lm.nb	0.0404
STAT1	1.15	0.41	0.0116	lm.nb	0.0409
SOX2	2.38	0.848	0.0116	lm.nb	0.0409
MKI67	1.18	0.421	0.0117	lm.nb	0.0411
TIGIT	1.92	0.687	0.012	lm.nb	0.0418
HIF1A	-1.02	0.368	0.0122	lm.nb	0.0423
HES1	1.11	0.4	0.0122	lm.nb	0.0423
FCGRT	1.28	0.463	0.0128	lm.nb	0.0437
MMP7	-2.39	0.866	0.0129	lm.nb	0.0437
CXCL14	-1.76	0.636	0.0129	lm.nb	0.0437
CXCL5	-4.06	1.47	0.0129	loglinear	0.0437
CD2	1.14	0.412	0.0131	lm.nb	0.044
COL6A3	-1.03	0.377	0.0134	lm.nb	0.0449
FZD8	2.03	0.741	0.0139	Wald	0.0463
CD14	1.37	0.504	0.014	lm.nb	0.0463
CXCL3	-1.65	0.608	0.0141	lm.nb	0.0467
IL1R2	2.28	0.841	0.0143	lm.nb	0.0469
NDUFA4L2	2.02	0.748	0.0148	lm.nb	0.0483

Differentially expressed genes (DEGs) that are upregulated in (A) $HPV16^{+}IR^{+}$ compared to $HPV16^{+}IR^{-}$ OPSCC, (B) $HPV16^{+}IR^{+}$ compared to HPV^{-} OPSCC and (C) $HPV16^{+}IR^{-}$ compared to HPV^{-} OPSCC are given as a positive log2 fold change value, while downregulated DEGs are indicated as a negative log2 fold change value. The standard deviation (SD), P-value and corrected P-value (method lm.nb, linear model.negative binomial or Wald) is given for each DEG.

Supplemental Table 5. Imaging mass cytometry clusters and superclusters.

Supercluster number	Supercluster name	Cluster number	Cluster name
sc01	HLADR+ tumor cell	**c11**	11_HLADR+_Ki67+_D240+_P16+_Bcat+_Ker+_tumor_cell
		c23	23_HLADR+_Bcat+_Ker+_tumor_cell
sc02	HLADR-Ki67+ tumor cell	**c26**	26_Ki67+_D240+_TGFb+_Bcat+_Ker+_tumor_cell
		c28	28_Ki67+_Bcat+_Ker+_tumor_cell
		c30	30_Ki67+_D240+_P16+_Bcat+_Ker+_tumor_cell
		c31	31_Ki67+_TGFb+_P16+_Bcat+_Ker+_tumor_cell
sc03	HLADR-Ki67- tumor cell	**c07**	07_CD103+_Bcat+_Ker+_tumor_cell
		c24	24_P16+_Bcat+_Ker+_tumor_cell
		c25	25_D240+_Bcat+_Ker+_tumor_cell
		c27	27_TGFb+_Bcat+_Ker+_tumor_cell
		c40	40_VISTA+_CD103+_Bcat+_Ker+_tumor_cell
		c46	46_PDL1+_P16+_Bcat+_Ker+_tumor_cell
		c47	47_IDO+_PDL1+_P16+_Bcat+_Ker+_tumor_cell
		c50	50_Caspase+_Bcat+_Ker+_tumor_cell
sc04	CD3+CD4+FOXP3- T cell	**c01**	01_CD3+_CD4+_CD7+_ICOS+_CD45ro+_T_cell
		c05	05_CD3+_CD4+_VISTA+_CD73+_CD38+_CD45ro+_T_cell
		c14	14_CD3+_CD4+_CD7+_CD45ro+_T_cell
		c34	34_CD3+_CD4+_CD7+_CD73+_CD38+_TGFb+_CD45ro+_T_cell
		c35	35_CD3+_CD4+_CD7+_CD73+_TGFb+_CD45ro+_T_cell
		c37	37_CD3+_CD4+_CD7+_ICOS+_CD103+_D240+_CD45ro+_T_cell
sc05	CD3+CD4+FOXP3+ Treg	**c42**	42_CD3+_CD4+_CD7+_FOXP3+_CD45ro+_D240+_Treg
		c43	43_CD3+_CD4+_CD7+_FOXP3+_ICOS+_CD45ro+_Treg
sc06	CD3+CD8+ T cell	**c03**	03_CD3+_CD8+_CD4+_CD57+_CD7+_CD45ro+_T_cell
		c04	04_CD3+_CD8+_CD7+_CD103+_CD45ro+_T_cell
		c36	36_CD3+_CD8+_CD7+_TGFb+_CD45ro+_T_cell
sc07	CD20+HLADR+ B cell	**c02**	02_CD20+_HLADR+_CD57+_ CD45ro+_ B_cell
		c41	41_CD20+_HLADR+_Ki67+_CD45+_B_cell
sc08	CD56+ NK cell	**c08**	08_CD56+_CD73+_VISTA+_NK_cell
sc09	CD3-CD7+ ILC	**c06**	06_CD7+_CD73+_TGFb+_ILC
sc10	CD11b+CD15+ granulocyte	**c48**	48_CD11b+_CD15+_VISTA+_CD45ro+_granulocyte
		c49	49_CD11b+_CD15+_CD45ro+_granulocyte
sc11	CD11c+CD14+HLADR+ DC	**c12**	12_CD11c+_CD14+_HLADR+_D240+_CD45ro+_DC
		c13	13_CD11c+_CD14+_HLADR+_CD45ro+_DC
sc12	CD68+CD163- M1 macrophage	**c15**	15_CD68+_CD14+_CD204+_HLADR+_TGFb+_macrophage
		c32	32_CD68+_VISTA+_CD38+_CD31+_macrophage
		c38	38_CD68+_CD14+_CD204+_CD11c+_HLADR+_macrophage
sc13	CD68+CD163+ M2 macrophage	**c39**	39_CD68+_CD163+_CD14+_CD204+_CD11c+_HLADR+_macrophage
		c44	44_CD68+_CD163+_CD14+_CD11c+_HLADR+_VISTA+_macrophage
		c45	45_CD68+_CD163+_CD14+_VISTA+_CD38+_CD31+_macrophage
		c51	51_CD68+_CD163+_macrophage
sc14	CD68-CD14+HLADR+ myeloid cell	**c16**	16_CD14+_ CD204+_HLADR+_ CD45ro+_myeloid_cell
		c17	17_CD14+_HLADR+_CD73+_TGFb+_myeloid_cell
sc15	CD45ro+lin- memory immune cell	**c22**	22_CD45ro+_memory_immune_cell
		c29	29_HLADR+_CD45ro+_memory_immune_cell
sc16	Vim+lin- fibroblast	**c18**	18_TGFb+_Vim+_fibroblast
		c19	19_Vim+_fibroblast
		c20	20_Vim+_D240+_fibroblast
sc17	CD38+Vim+lin- stromal cell	**c21**	21_CD38+_stromal_cell
		c33	33_CD38+_CD31+_CD73+_TGFb+_stromal_cell
sc18	CD31+ blood vessel endothelial cell	**c09**	09_CD31+_CD73+_blood_vessel
		c10	10_CD31+_CD73+_TGFb+_blood_vessel

Supplemental Table 5. Continued.

Supercluster number	Supercluster name	Cluster number	Cluster name
sc19	D240+ tumor cell	**c11**	11_HLADR+_Ki67+_D240+_P16+_Bcat+_Ker+_tumor_cell
		c25	25_D240+_Bcat+_Ker+_tumor_cell
		c26	26_Ki67+_D240+_TGFb+_Bcat+_Ker+_tumor_cell
		c30	30_Ki67+_D240+_P16+_Bcat+_Ker+_tumor_cell
sc20	CD103+ tumor cell	**c07**	07_CD103+_Bcat+_Ker+_tumor_cell
		c40	40_VISTA+_CD103+_Bcat+_Ker+_tumor_cell
sc21	Ki67+ tumor cell	**c11**	11_HLADR+_Ki67+_D240+_P16+_Bcat+_Ker+_tumor_cell
		c26	26_Ki67+_D240+_TGFb+_Bcat+_Ker+_tumor_cell
		c28	28_Ki67+_Bcat+_Ker+_tumor_cell
		c30	30_Ki67+_D240+_P16+_Bcat+_Ker+_tumor_cell
		c31	31_Ki67+_TGFb+_P16+_Bcat+_Ker+_tumor_cell
sc22	CD3+FOXP3-TGFb+ T cell	**c34**	34_CD3+_CD4+_CD7+_CD73+_CD38+_TGFb+_CD45ro+_Th_cell
		c35	35_CD3+_CD4+_CD7+_CD73+_TGFb+_CD45ro+_T_cell
		c36	36_CD3+_CD8+_CD7+_TGFb+_CD45ro+_Tc_cell
sc23	CD11c+ cell	**c12**	12_CD11c+_CD14+_HLADR+_D240+_CD45ro+_DC
		c13	13_CD11c+_CD14+_HLADR+_CD45ro+_DC
		c38	38_CD68+_CD14+_CD204+_CD11c+_HLADR+_macrophage
sc24	CD38+CD31+ stromal cell	**c32**	32_CD68+_VISTA+_CD38+_CD31+_macrophage
		c33	33_CD38+_CD31+_CD73+_TGFb+_stromal_cell
		c45	45_CD68+_CD163+_CD14+_VISTA+_CD38+_CD31+_macrophage
sc25	CD103+ T cell	**c37**	37_CD3+_CD4+_CD7+_ICOS+_CD103+_D240+_CD45ro+_Th_cell
		c04	04_CD3+_CD8+_CD7+_CD103+_CD45ro+_Tc_cell
sc26	ICOS+ T cell	**c01**	01_CD3+_CD4+_CD7+_ICOS+_CD45ro+_Th_cell
		c37	37_CD3+_CD4+_CD7+_ICOS+_CD103+_D240+_CD45ro+_Th_cell
		c43	43_CD3+_CD4+_CD7+_FOXP3+_ICOS+_CD45ro+_Treg
sc27	TGFb+ myeloid cell	**c15**	15_CD68+_CD14+_CD204+_HLADR+_TGFb+_macrophage
		c17	17_CD14+_HLADR+_CD73+_TGFb+_myeloid_cell
sc28	CD14+ myeloid cell	**c12**	12_CD11c+_CD14+_HLADR+_D240+_CD45ro+_DC
		c13	13_CD11c+_CD14+_HLADR+_CD45ro+_DC
		c15	15_CD68+_CD14+_CD204+_HLADR+_TGFb+_macrophage
		c38	38_CD68+_CD14+_CD204+_CD11c+_HLADR+_macrophage
		c39	39_CD68+_CD163+_CD14+_CD204+_CD11c+_HLADR+_macrophage
		c44	44_CD68+_CD163+_CD14+_CD11c+_HLADR+_VISTA+_macrophage
		c45	45_CD68+_CD163+_CD14+_VISTA+_CD38+_CD31+_macrophage
		c16	16_CD14+_ CD204+_HLADR+_ CD45ro+_myeloid_cell
		c17	17_CD14+_HLADR+_CD73+_TGFb+_myeloid_cell

Cluster name is based on the markers that are expressed by that cluster, indicating that that cluster is negative for all other tested markers that are not mentioned in the cluster name.

Supplemental Table 6. Single cell sequencing counts per identified cluster.

	H143	H197	H205	H149	H182	H208	H211	H141	H160	H176	H185	H188	H68
Cluster	HPV-	HPV-	HPV-	HPV+ IR-	HPV+ IR-	HPV+ IR-	HPV+ IR-	HPV+ IR+	HPV+ IR+	HPV+ IR+	HPV+ IR+	HPV+ IR+	HPV+ IR+
CD8_0	31*	66	10	5	45	10	15	19	73	50	302	184	49
CD8_1	276	7	10	10	90	8	23	63	81	70	54	18	64
CD8_2	446	2	5	2	12	0	6	8	32	10	14	6	1
CD8_3	0	71	6	0	7	41	2	0	10	83	65	18	212
CD8_4	9	8	4	17	96	2	11	7	9	33	81	205	33
CD8_5	7	87	9	10	15	15	10	21	11	30	90	132	15
CD8_6	0	15	2	1	9	316	2	2	5	15	17	24	22
CD8_7	1	1	1	9	11	3	4	12	1	12	7	40	305
CD8_8	0	0	0	0	8	5	4	2	3	4	8	26	255
CD8_9	2	2	1	0	0	5	3	0	1	101	0	0	151
CD8_10	0	16	3	0	2	45	0	1	1	10	13	4	38
CD8_11	1	19	1	0	3	5	1	0	6	1	0	2	0
CD4_0	2	0	4	202	51	5	28	7	1	33	40	324	224
CD4_1	103	12	53	87	82	7	78	48	251	23	136	8	11
CD4_2	3	17	12	9	98	172	28	27	10	33	14	82	379
CD4_3	203	0	43	74	52	1	175	96	104	2	16	5	3
CD4_4	17	2	15	11	15	16	112	516	13	9	8	8	22
CD4_5	16	61	19	47	81	7	32	34	24	45	113	239	42
CD4_6	9	3	33	309	54	0	5	19	8	11	85	16	8
CD4_7	19	46	16	15	40	41	44	22	87	113	53	21	10
CD4_8	11	99	8	8	26	41	7	10	16	34	38	90	100
CD4_9	38	6	14	3	54	19	74	39	93	95	7	3	14
CD4_10	2	3	0	0	0	2	0	2	6	29	0	4	107
Treg_0	4	67	8	17	46	23	31	71	31	58	61	101	116
Treg_1	3	20	6	6	41	94	7	5	7	42	15	51	102
Treg_2	0	7	0	0	4	181	4	10	0	7	0	7	13
Treg_3	0	141	1	0	4	3	0	0	0	2	2	1	3
Treg_4	0	16	3	3	18	38	8	5	10	20	5	8	21
Treg_5	0	0	0	0	0	5	0	0	0	25	1	1	36
Tother_0	18	0	4	0	23	2	13	10	8	2	9	11	3
Tother_1	2	0	7	0	11	1	1	4	0	0	0	3	5
Tother_2	1	0	1	3	5	1	1	2	1	0	0	3	0
NK_0	2	21	21	46	149	14	20	16	28	78	59	97	272
NK_1	1	222	8	6	46	34	14	11	42	55	288	35	22
NK_2	0	12	1	1	9	586	0	22	0	9	6	5	11
NK_3	2	5	13	7	54	22	40	19	37	16	13	8	8
NK_4	0	146	5	1	13	18	4	4	6	8	6	7	14
NK_5	0	0	1	0	0	2	0	0	1	36	2	0	35

* Number of cells identified per patient in each cluster.

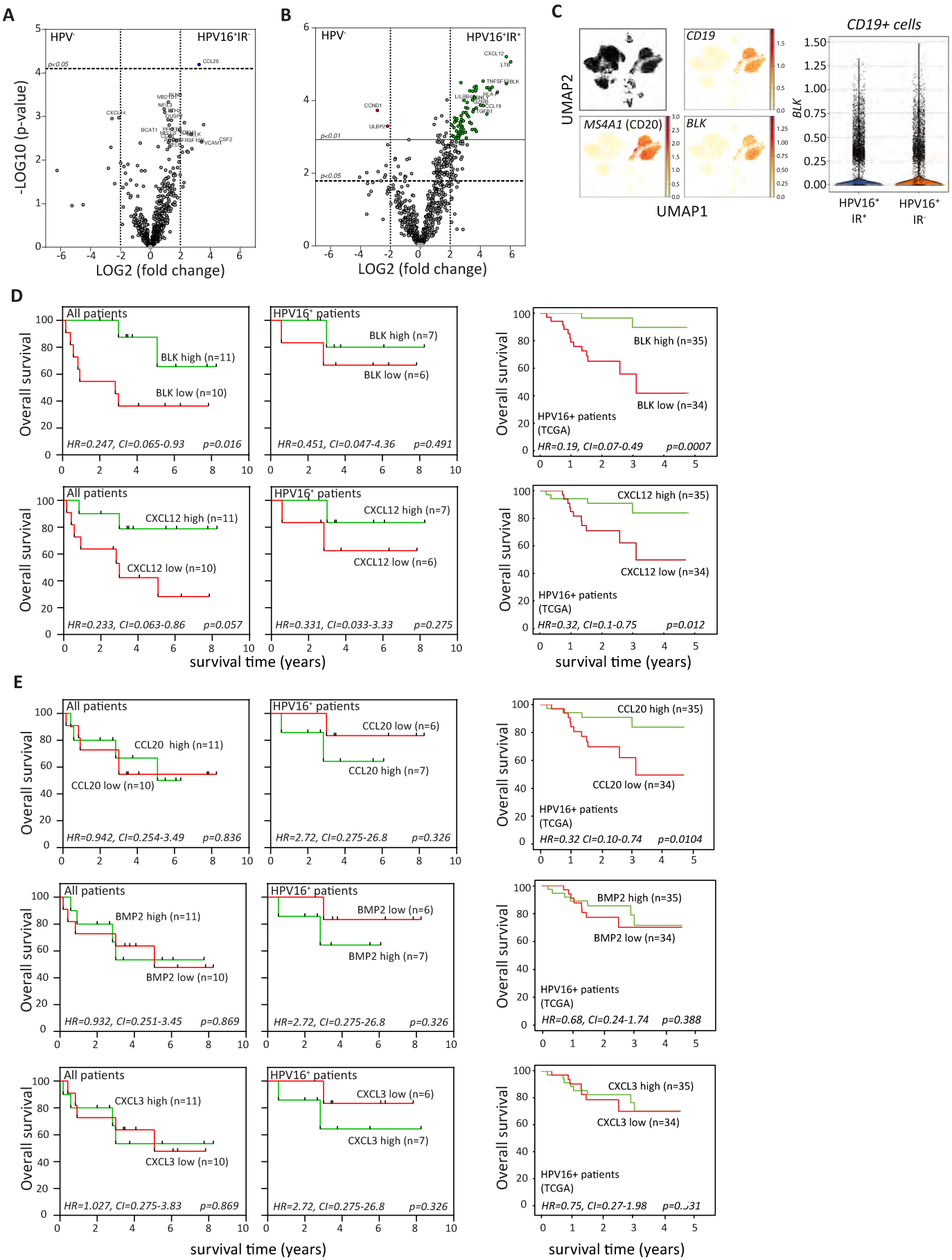
A
HPV⁻
HPV16⁺IR⁻
p<0.05
CCL20
-LOG10 (p-value)
LOG2 (fold change)
B
HPV⁻
HPV16⁺IR⁺
CXCL12
LTB
TNFSF13B
BLK
CCND1
ULBP2
CCL19
p<0.01
p<0.05
LOG2 (fold change)
C
UMAP2
UMAP1
CD19
MS4A1 (CD20)
BLK
CD19+ cells
BLK
HPV16⁺ IR⁺
HPV16⁺ IR⁻
D
All patients
BLK high (n=11)
BLK low (n=10)
HR=0.247, CI=0.065-0.93 p=0.016
HPV16⁺ patients
BLK high (n=7)
BLK low (n=6)
HR=0.451, CI=0.047-4.36 p=0.491
BLK high (n=35)
BLK low (n=34)
HPV16+ patients
(TCGA)
HR=0.19, CI=0.07-0.49 p=0.0007
CXCL12 high (n=11)
CXCL12 low (n=10)
HR=0.233, CI=0.063-0.86 p=0.057
CXCL12 high (n=7)
CXCL12 low (n=6)
HR=0.331, CI=0.033-3.33 p=0.275
CXCL12 high (n=35)
CXCL12 low (n=34)
HR=0.32, CI=0.1-0.75 p=0.012
Overall survival
survival time (years)
E
CCL20 high (n=11)
CCL20 low (n=10)
HR=0.942, CI=0.254-3.49 p=0.836
CCL20 low (n=6)
CCL20 high (n=7)
HR=2.72, CI=0.275-26.8 p=0.326
CCL20 high (n=35)
CCL20 low (n=34)
HR=0.32 CI=0.10-0.74 p=0.0104
BMP2 high (n=11)
BMP2 low (n=10)
HR=0.932, CI=0.251-3.45 p=0.869
BMP2 low (n=6)
BMP2 high (n=7)
HR=2.72, CI=0.275-26.8 p=0.326
BMP2 high (n=35)
BMP2 low (n=34)
HR=0.68, CI=0.24-1.74 p=0.388
CXCL3 high (n=11)
CXCL3 low (n=10)
HR=1.027, CI=0.275-3.83 p=0.869
CXCL3 low (n=6)
CXCL3 high (n=7)
HR=2.72, CI=0.275-26.8 p=0.326
CXCL3 high (n=35)
CXCL3 low (n=34)
HR=0.75, CI=0.27-1.98 p=0.731

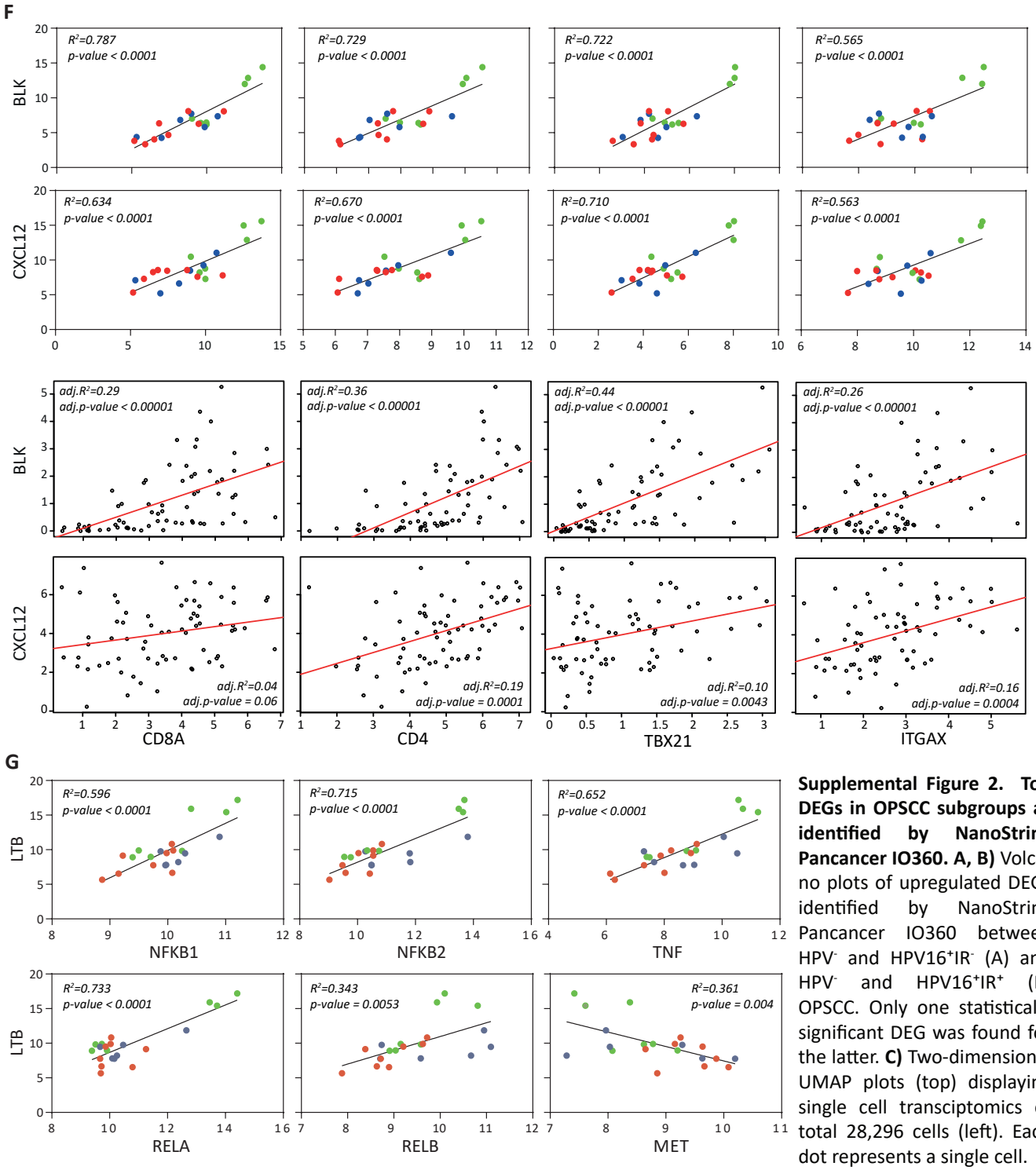

Supplemental Figure 2. Top DEGs in OPSCC subgroups as identified by NanoString Pancancer IO360. A, B) Volcano plots of upregulated DEGs identified by NanoString Pancancer IO360 between HPV⁻ and HPV16⁺IR⁻ (A) and HPV⁻ and HPV16⁺IR⁺ (B) OPSCC. Only one statistically significant DEG was found for the latter. **C)** Two-dimensional UMAP plots (top) displaying single cell transciptomics of total 28,296 cells (left). Each dot represents a single cell. Expression levels of *CD19*, *MS4A1* (CD20) and *BLK* are depicted in color code. Violin plot (right) displaying expression of *BLK* within B cells from HPV16⁺IR⁺ (blue; left) and HPV16⁺IR⁻ (orange; right) OPSCC. **D)** Kaplan-Meier survival curves based on high/low *BLK* or *CXCL12* expression (classification based on median *BLK* or *CXCL12* expression) upregulated in HPV16⁺IR⁺ compared to HPV16⁺IR⁻ OPSCC patients for all OPSCC patients analyzed by Nanostring Pancancer IO360 (n=21; left), for the HPV16⁺ patients within this cohort (n=13; middle), and for a large independent TCGA cohort of HPV16⁺ OPSCC (n=69; right). **E)** Kaplan-Meier survival curves based on high/low expression of the top 3 DEGs (*CCL20, BMP2 and CXCL3)* upregulated in HPV16⁺IR⁻ compared to HPV16⁺IR⁺ OPSCC patients for all OPSCC patients analyzed by Nanostring Pancancer IO360 (n=21, left), for the HPV16⁺ patients within this cohort (n=13; middle), and for a large independent TCGA cohort of HPV16⁺ OPSCC (n=69; right). **F)** Linear regression analysis of top upregulated DEGs *BLK* and *CXCL12* in HPV16⁺IR⁺ compared to HPV16⁺IR⁻ OPSCC versus cell type profiles of CD8 (*CD8A*), CD4, Tbet⁺ T cells (*TBX21*) and DC (*ITGAX*, CD11c). Upper 2 panels display all OPSCC patients analyzed by Nanostring Pancancer IO360 (n=21). Each patient is represented by a colored dot: HPV⁻ (red), HPV16⁺IR⁻ (blue) and HPV16⁺IR⁺ (green). The lower 2 panels show the regression analysis of the 69 HPV16⁺ OPSCC patients of the independent TCGA cohort. **G)** Linear regression analysis of *LTB* versus indicated genes involved in tumor cell migration (metastases) and cell activation.

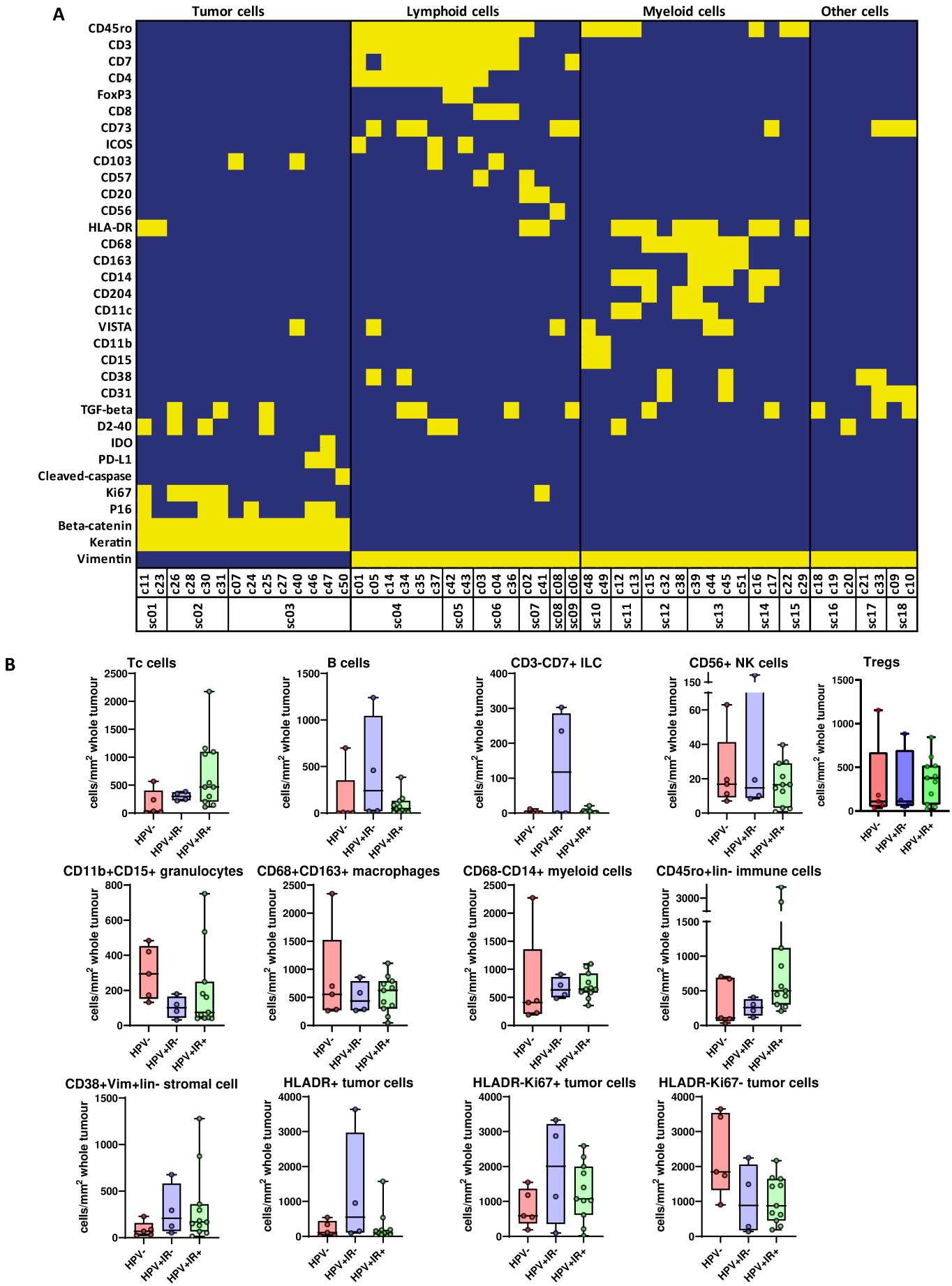

Supplemental Figure 3. Imaging mass cytometry identified (super)clusters in the TME of OPSCC.
Using the unsupervised HSNE-based clustering program Cytosplore, 51 individual cell clusters were identified. **A)** Heatmap of the verified markers expressed in the identified clusters (c01-c51), and the manual grouping into mutually exclusive superclusters (sc01-sc18). **B)** Quantitative comparisons of the remaining 13 of the 18 superclusters present in OPSCC. The three distinct OPSCC subgroups are indicated by different colors: HPV- red (n=5), HPV16+IR- blue (n=4) and HPV16+IR+ green (n=11). Boxplots with bars in box representing the median and interquartile range.

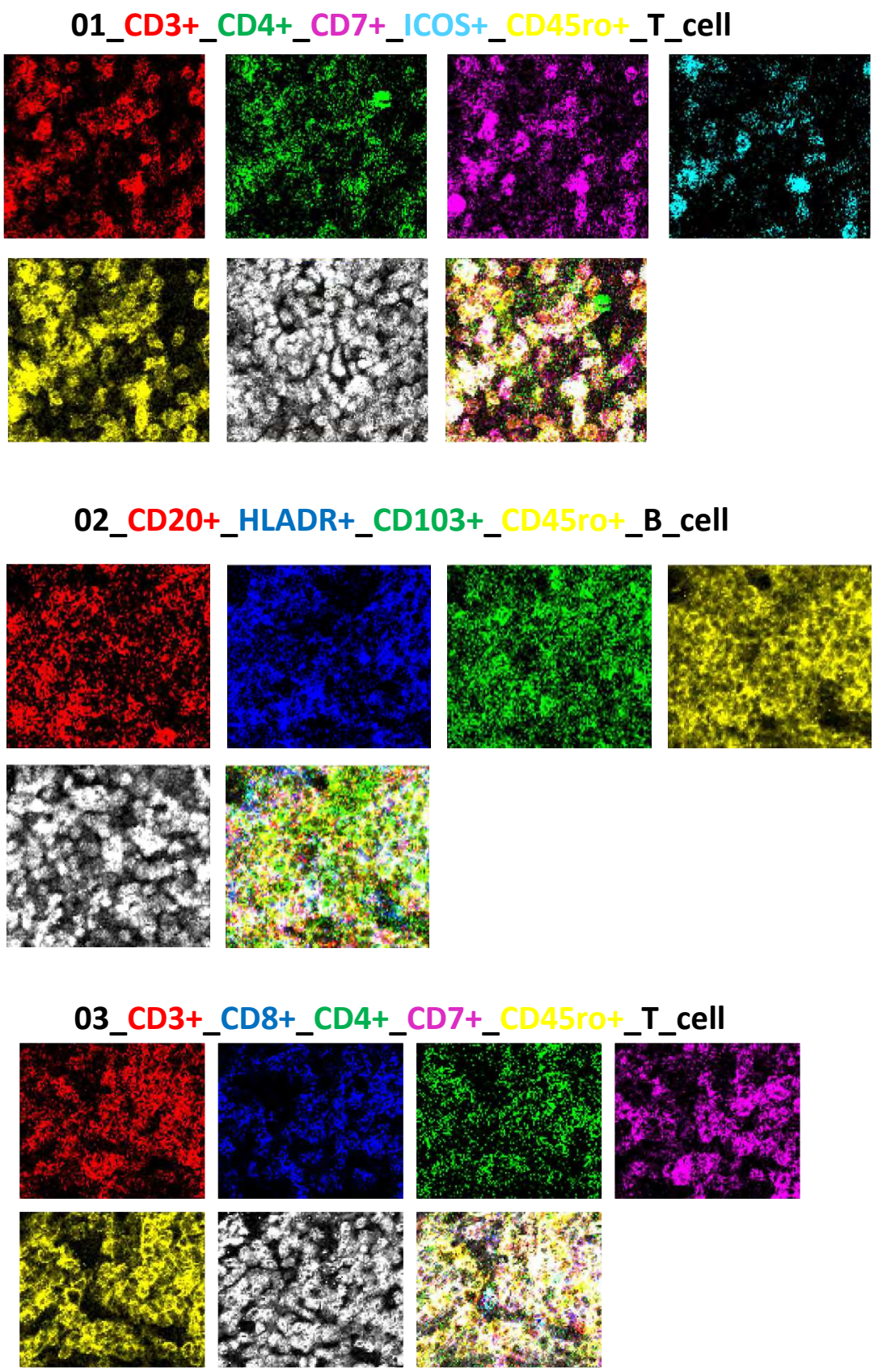

Supplemental Figure 4. Imaging mass cytometry images of the 51 identified clusters.
Representative images of cells of all 51 clusters, including separate images of all positive markers, including cell nuclei (DNA) consistently in white, and overlays for all clusters.

04_CD3+_CD8+_CD7+_CD103+_CD45ro+_T_cell

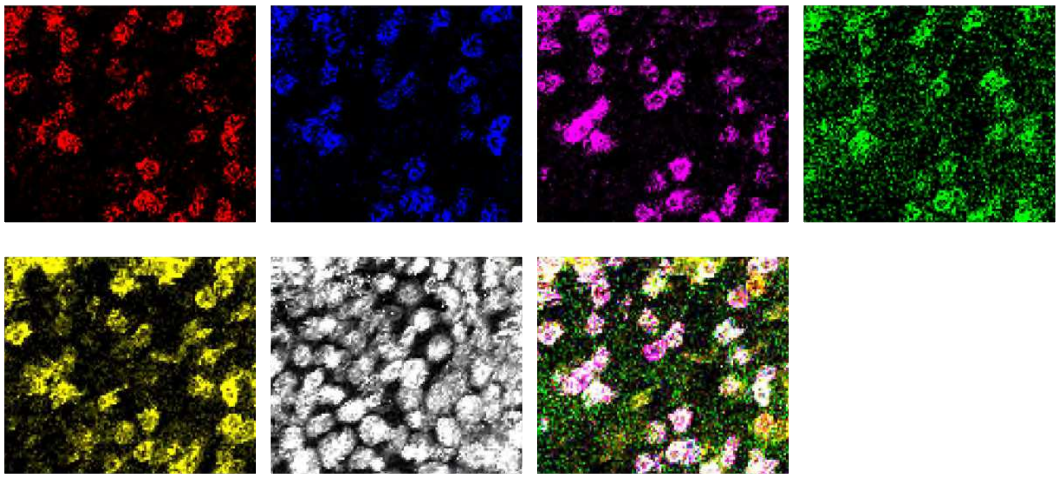

05_CD3+_CD4+_VISTA+_CD73+_CD38+_CD45ro+_T_cell

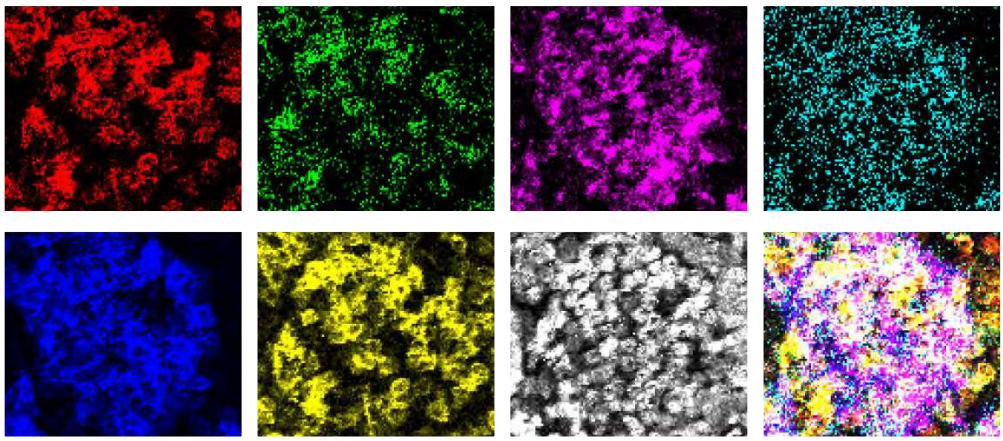

06_CD7+_CD73+_TGFb+_ILC

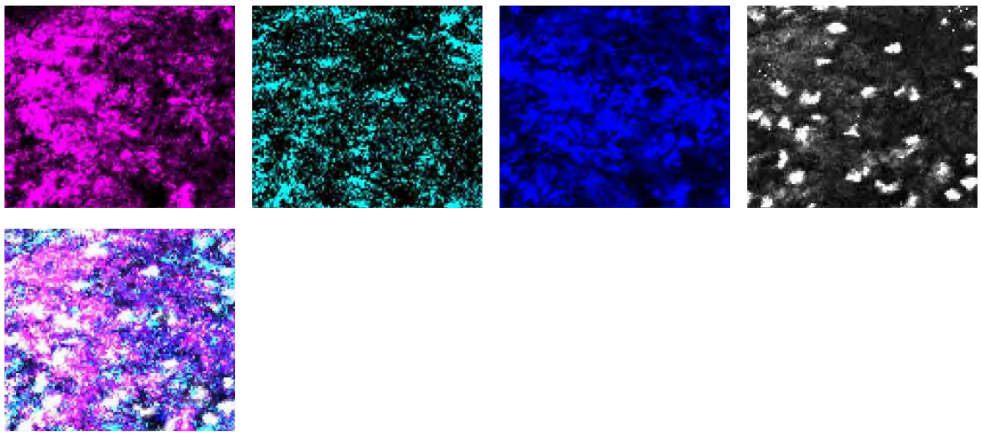

07_CD103+_Bcat+_Ker+_tumor_cell

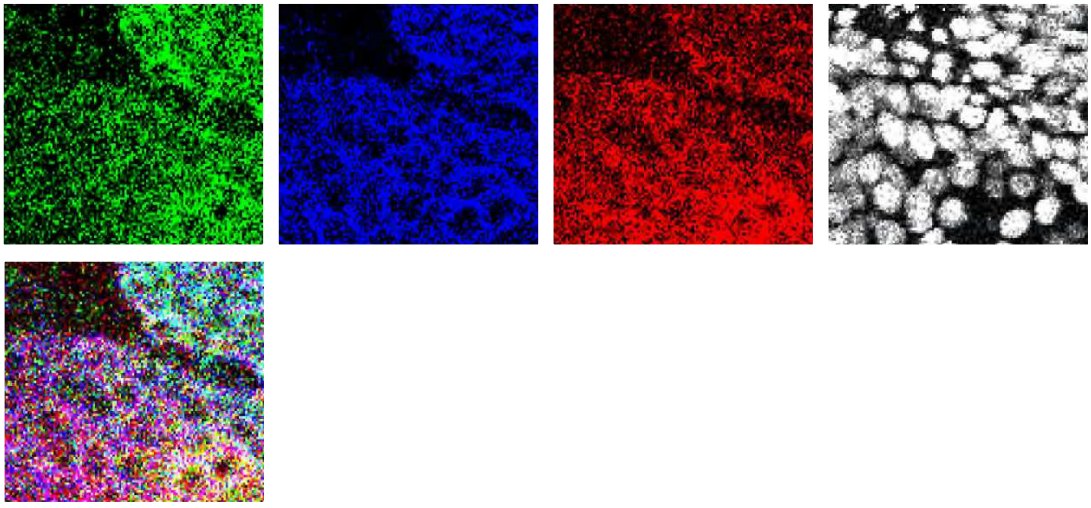

08_CD56+_CD73+_VISTA+_NK_cell

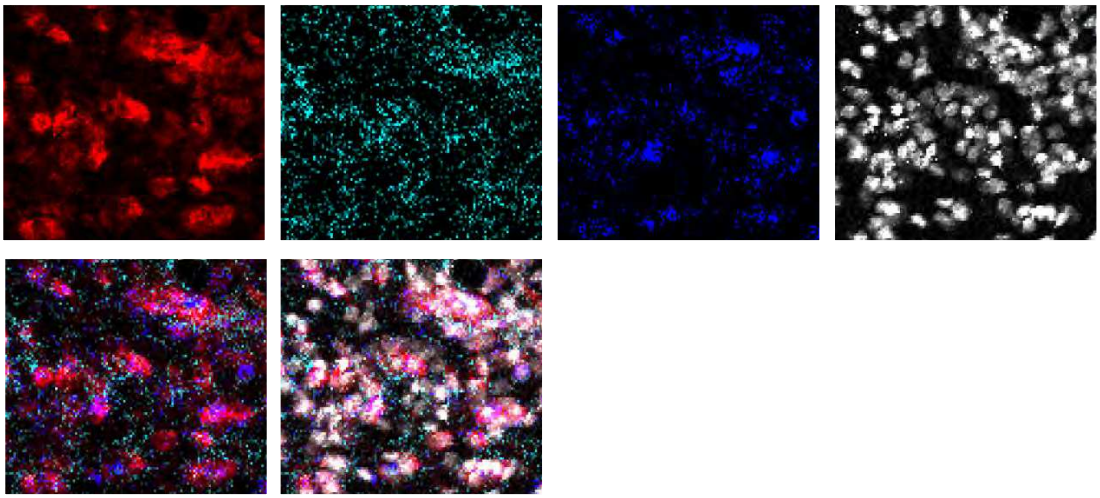

09_CD31+_CD73+_blood_vessel

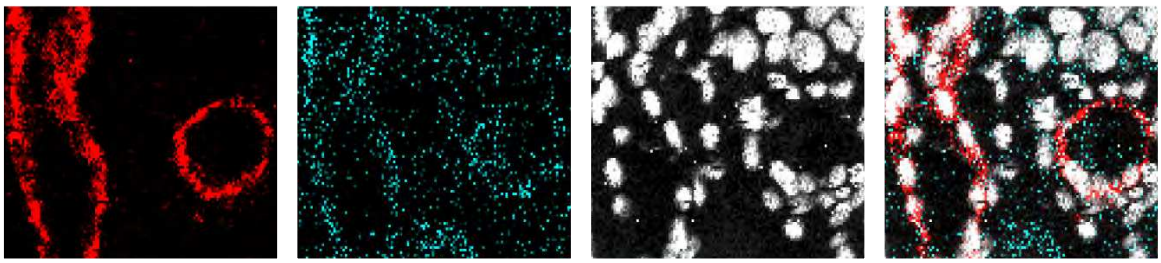

10_CD31+_CD73+_TGFb+_blood_vessel

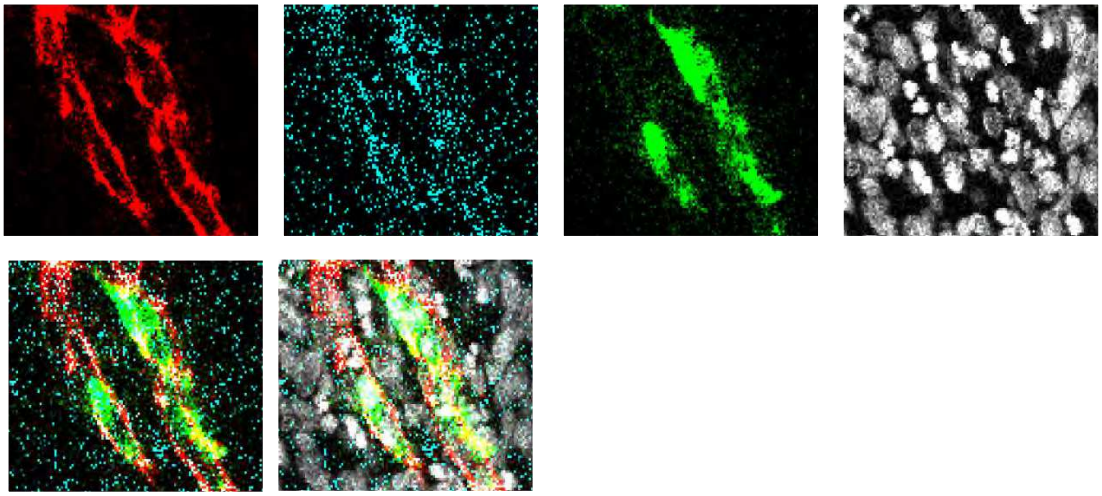

11_HLADR+_Ki67+_D240+_P16+_Bcat+_Ker+_tumor_cell

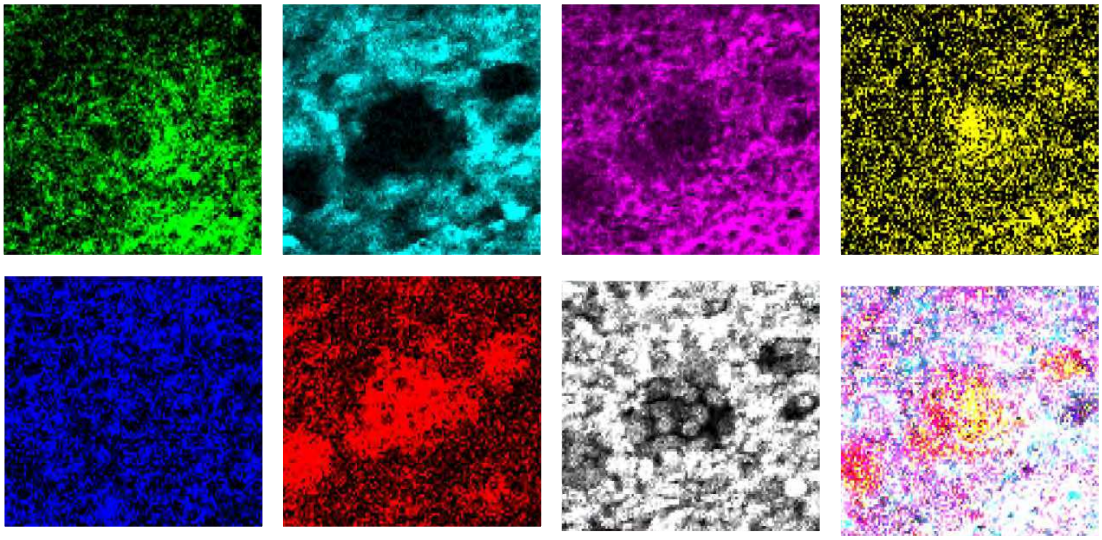

12_CD11c+_CD14+_HLADR+_D240+_CD45ro+_DC

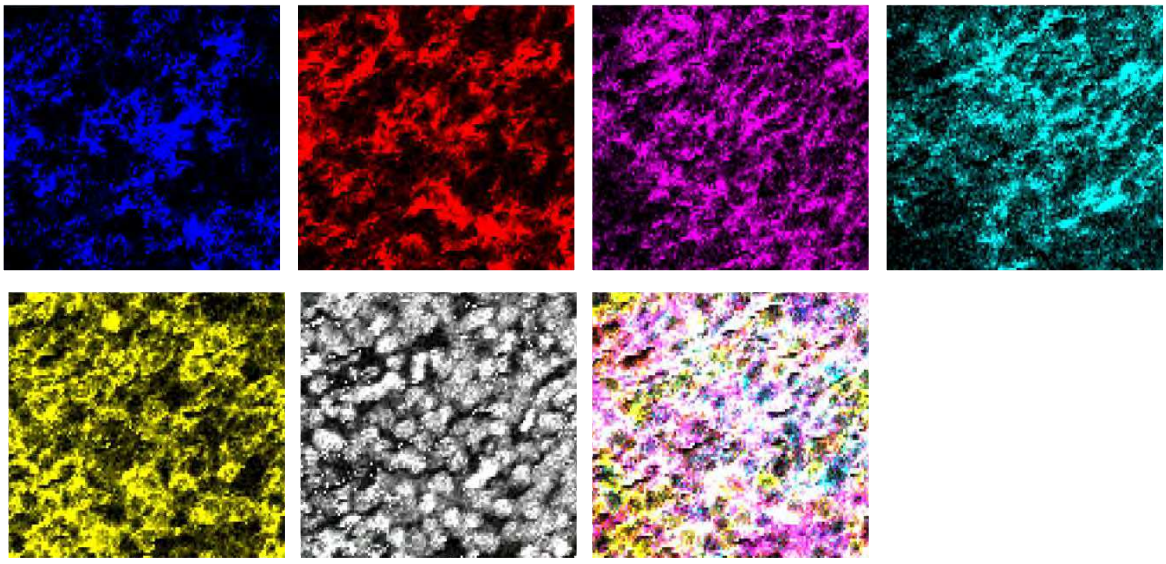

13_CD11c+_CD14+_HLADR+_CD45ro+_DC

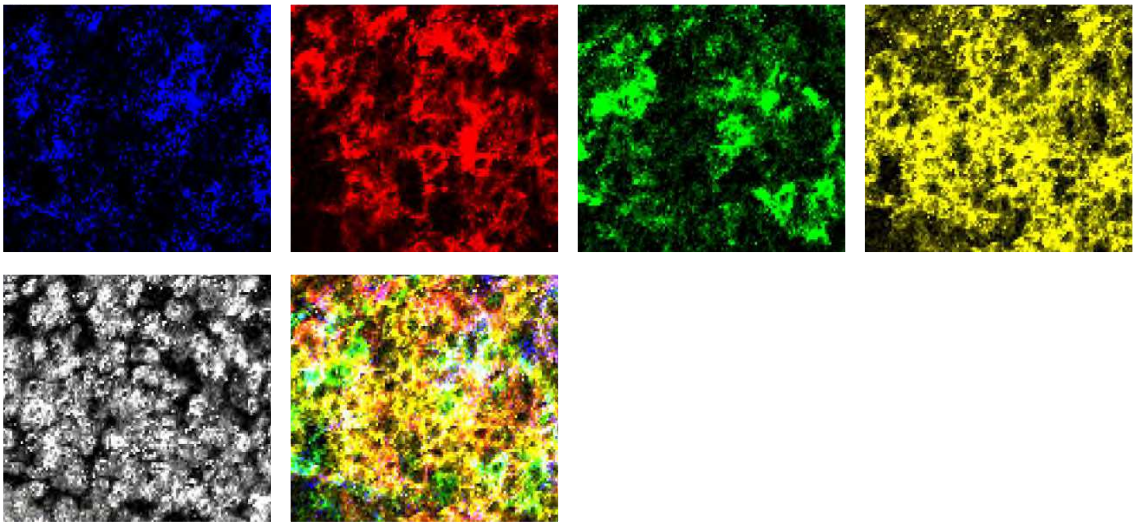

14_CD3+_CD4+_CD7+_CD45ro+_T_cell

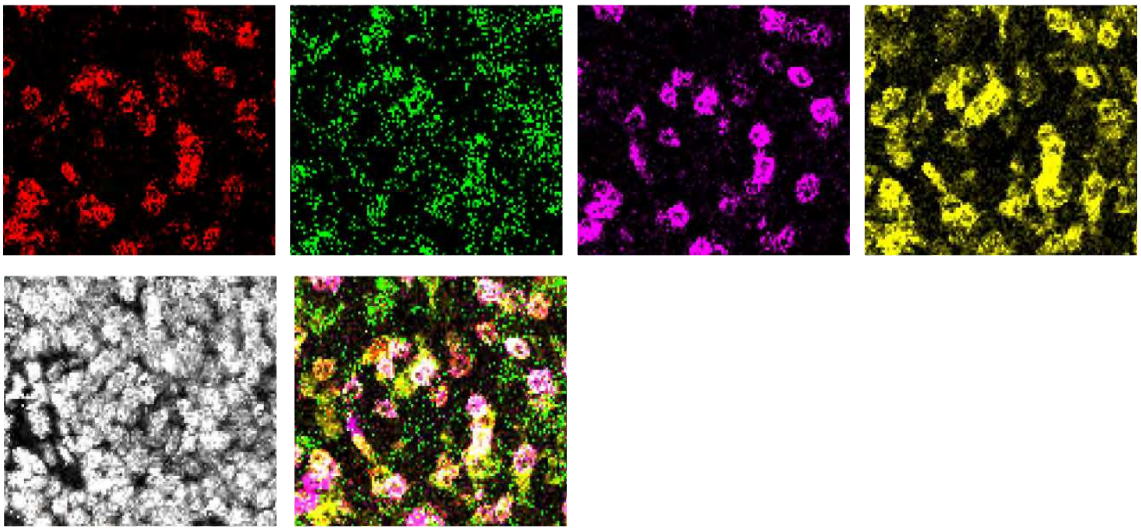

15_CD68+_CD14+_CD204+_HLADR+_TGFb+_macrophage

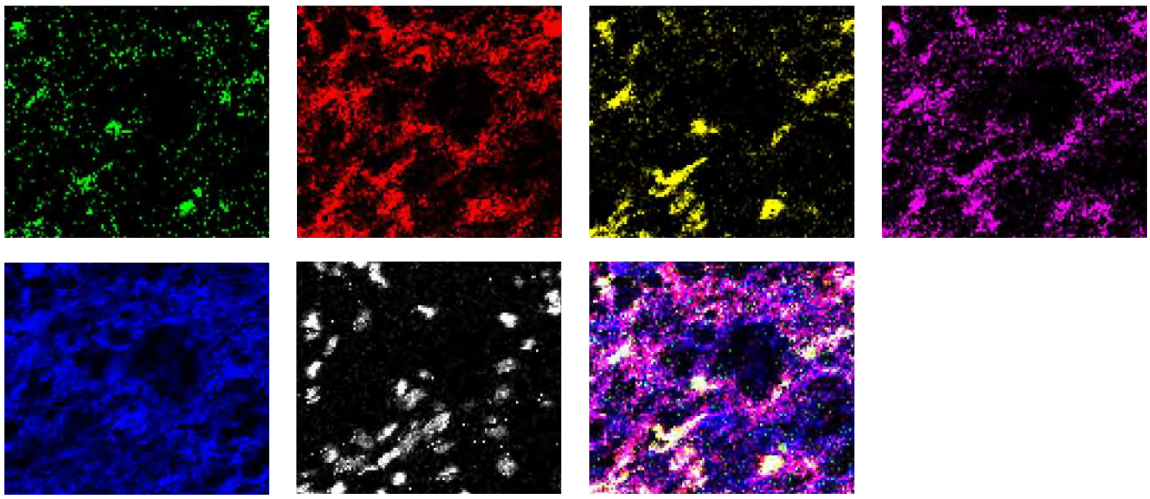

16_CD14+_ CD204+_HLADR+_ CD45ro+_myeloid_cell

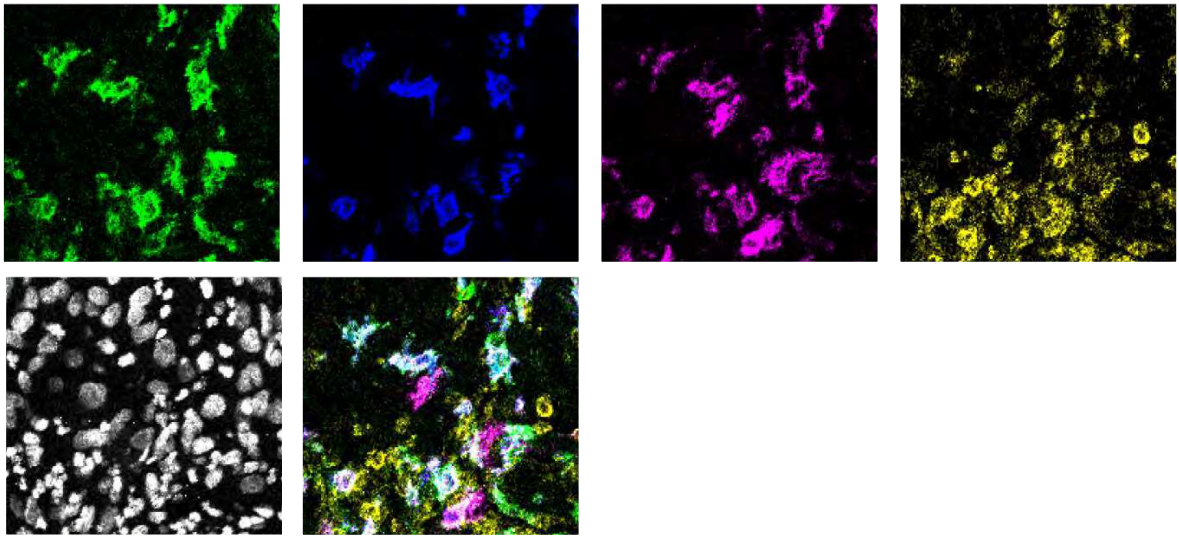

17_CD14+_HLADR+_CD73+_TGFb+_myeloid_cell

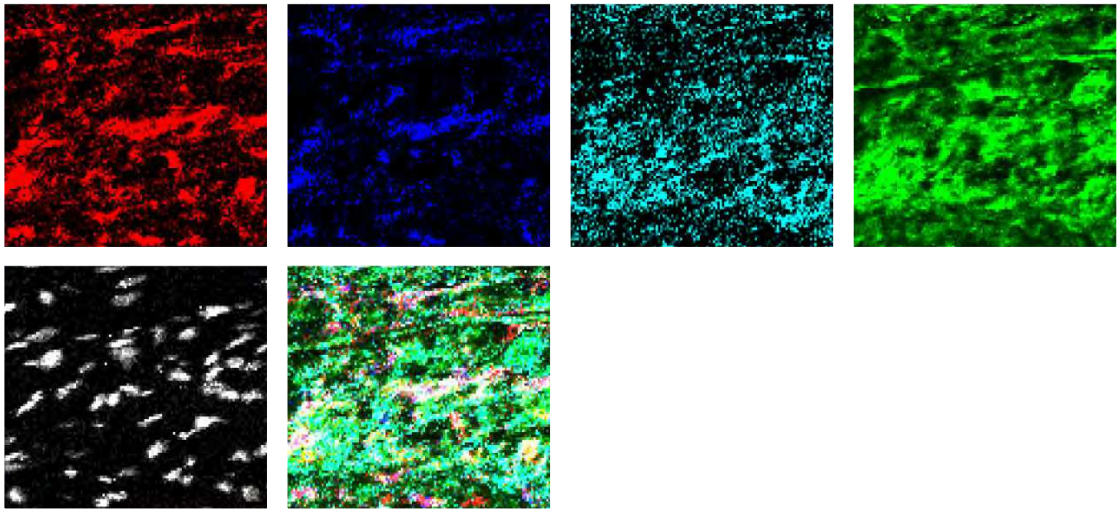

18_TGFb+_Vim+_fibroblast

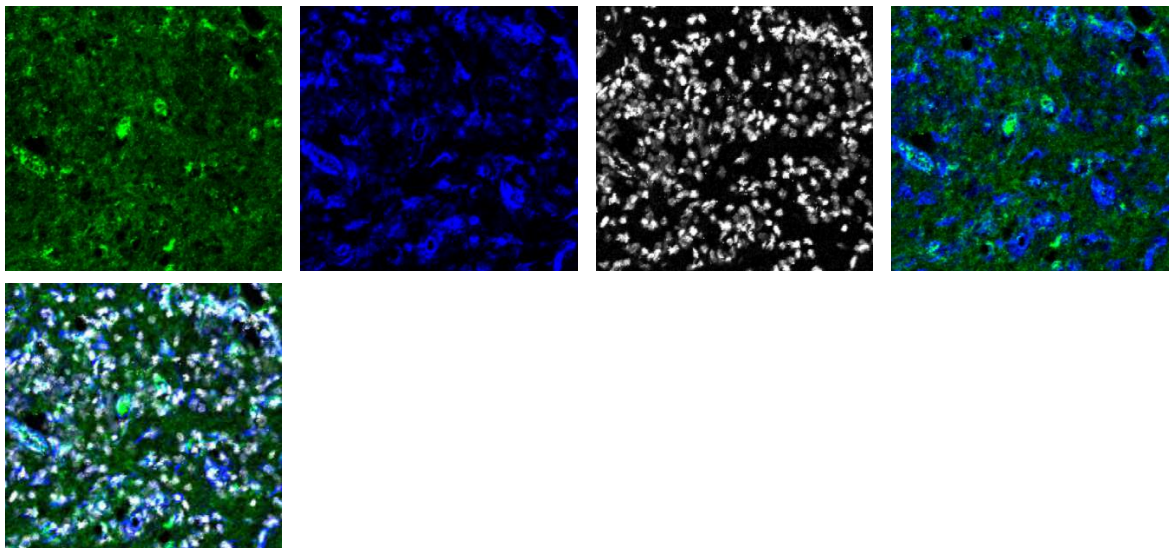

19_Vim+_fibroblast

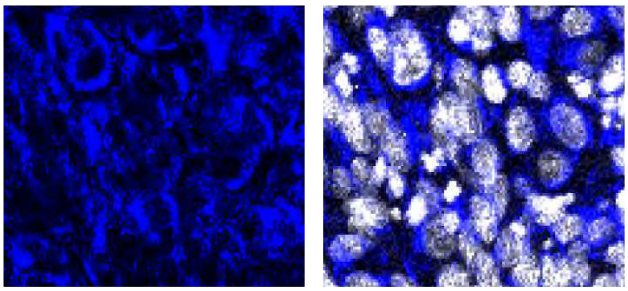

20_Vim+_D240+_fibroblast

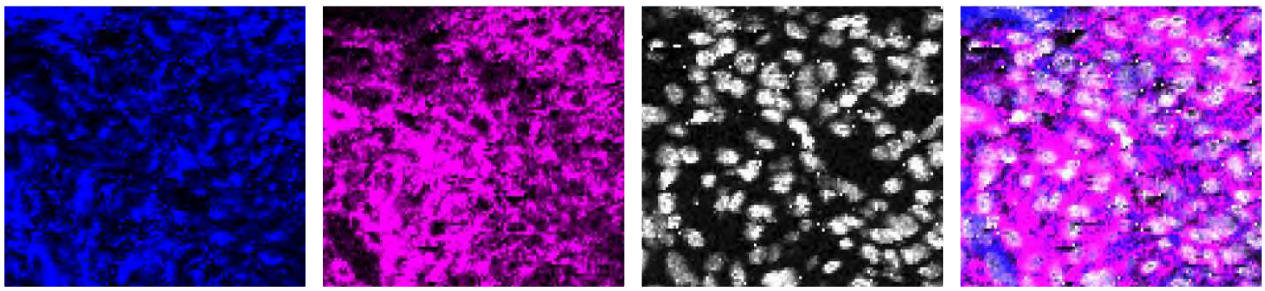

21_CD38+_stromal_cell

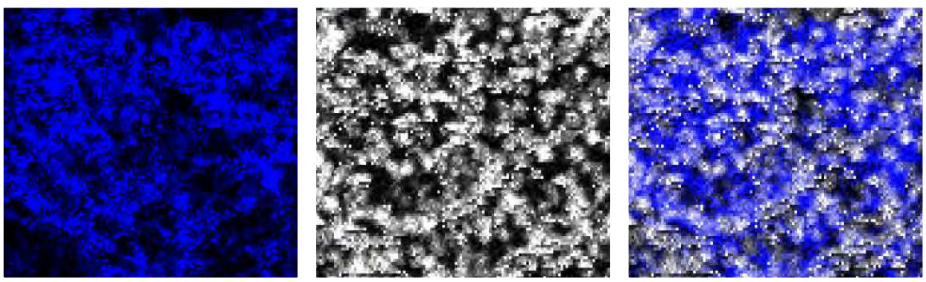

22_CD45ro+_memory_immune_cell

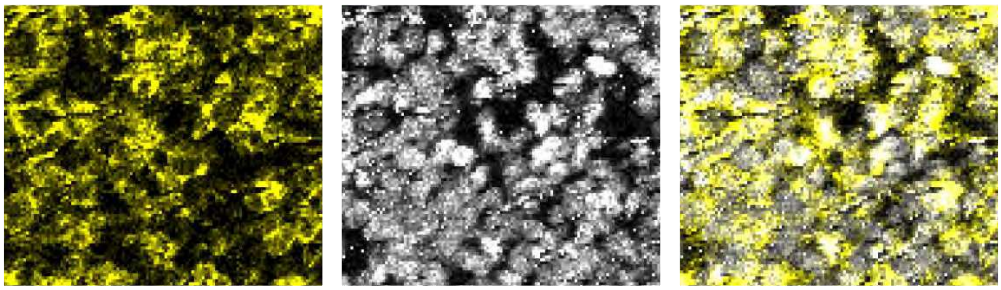

23_HLADR+_Bcat+_Ker+_tumor_cell

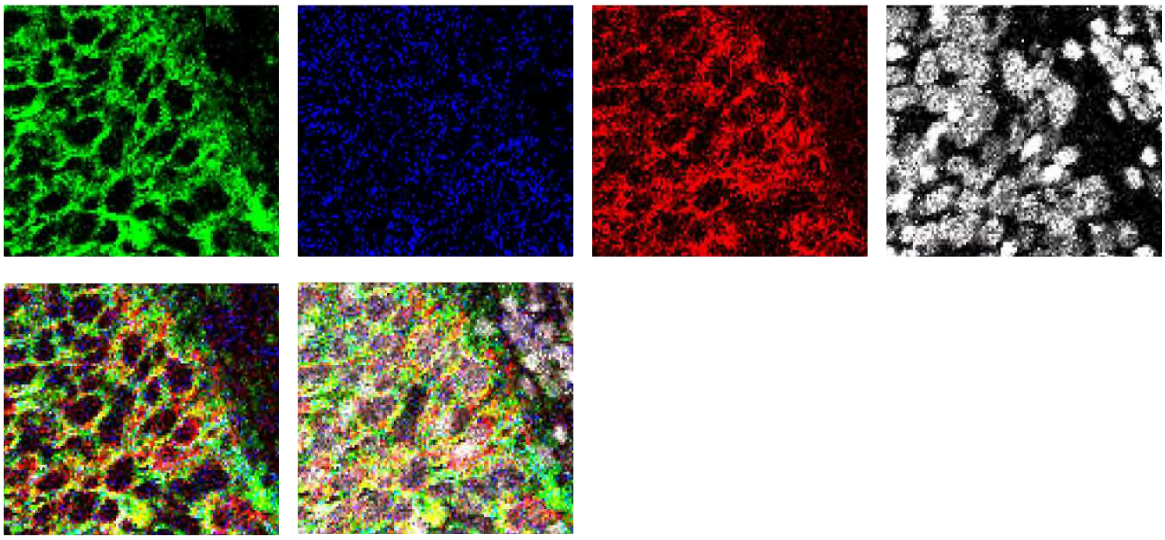

24_P16+_Bcat+_Ker+_tumor_cell

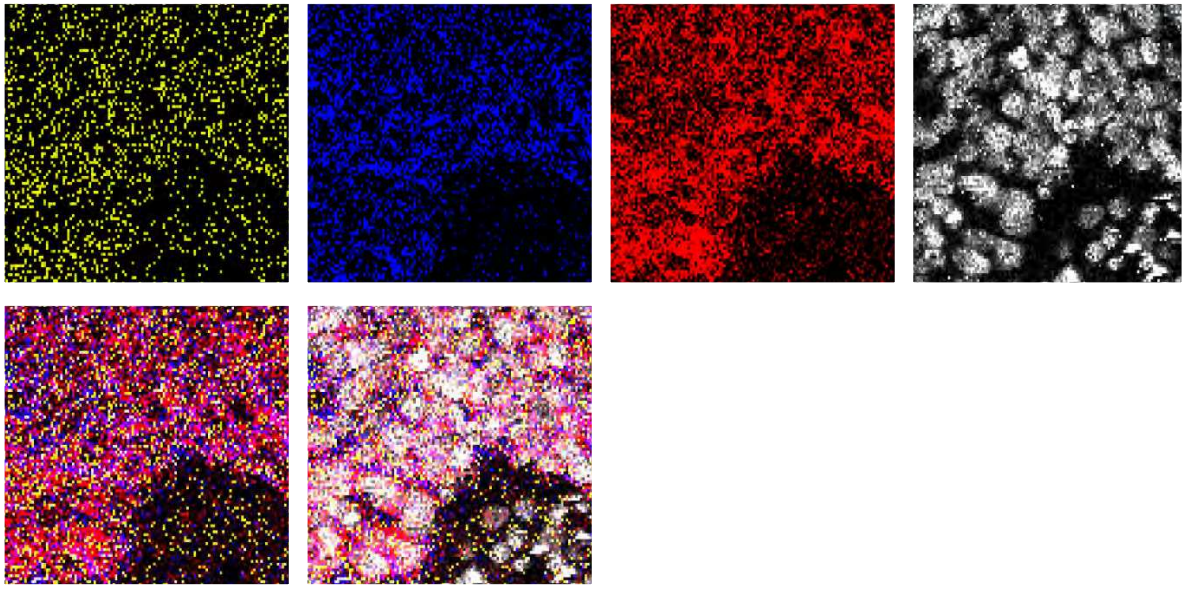

25_D240+_Bcat+_Ker+_tumor_cell

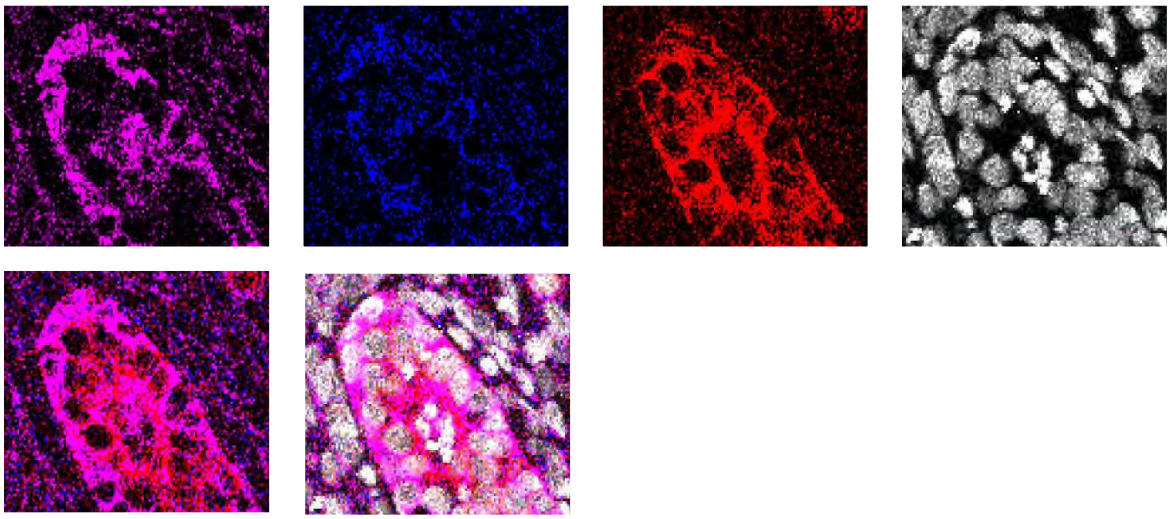

26_Ki67+_D240+_TGFb+_Bcat+_Ker+_tumor_cell

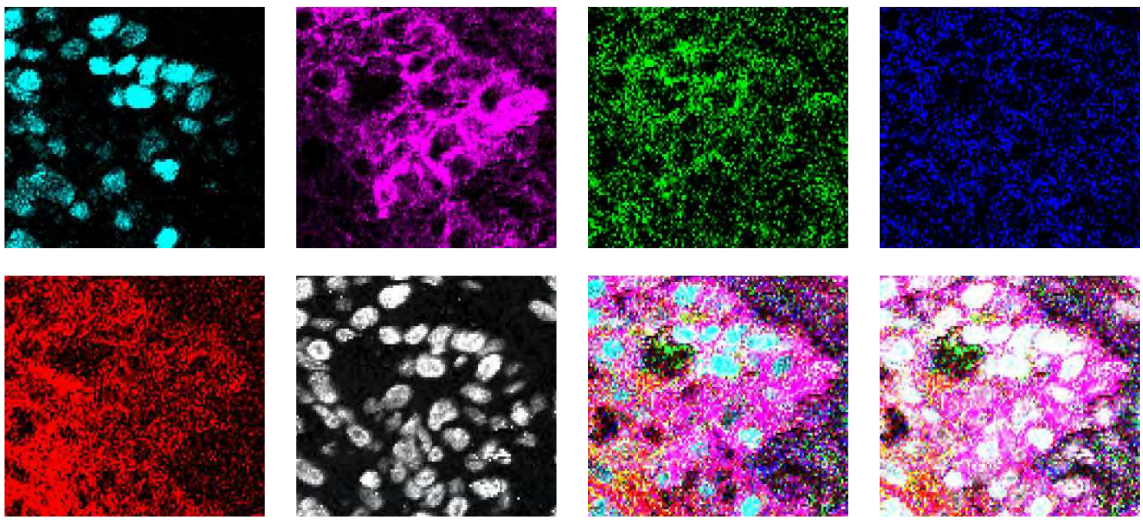

27_TGFb+_Bcat+_Ker+_tumor_cell

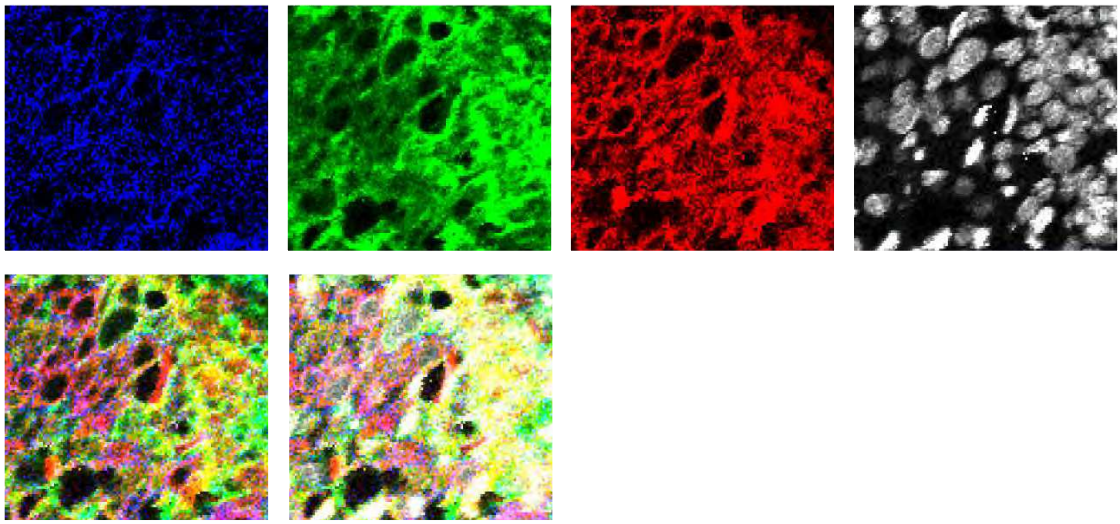

28_Ki67+_Bcat+_Ker+_tumor_cell

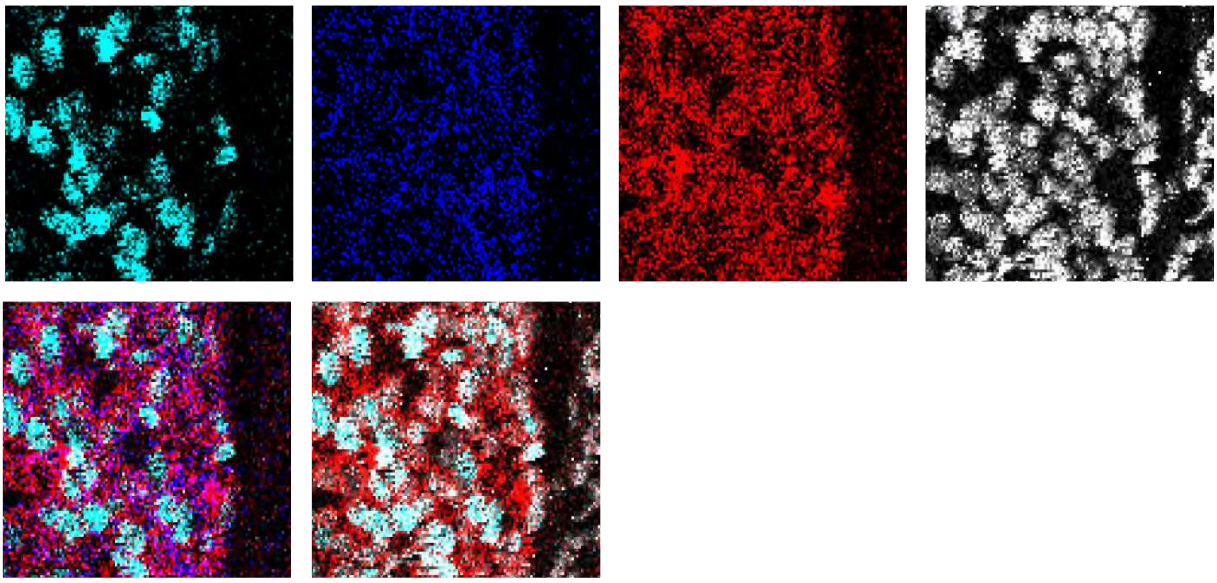

29_HLADR+_CD45ro+_memory_immune_cell

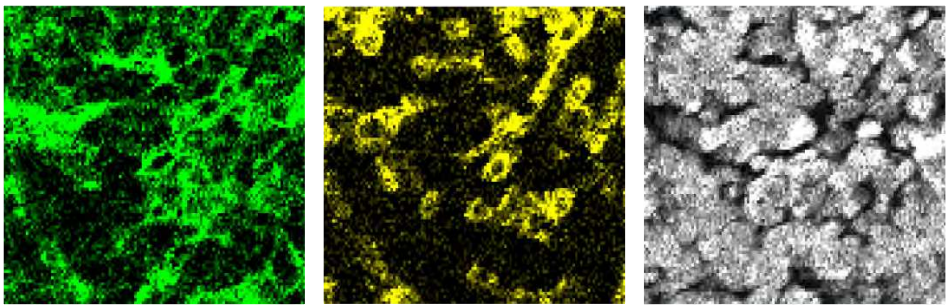

30_Ki67+_D240+_P16+_Bcat+_Ker+_tumor_cell

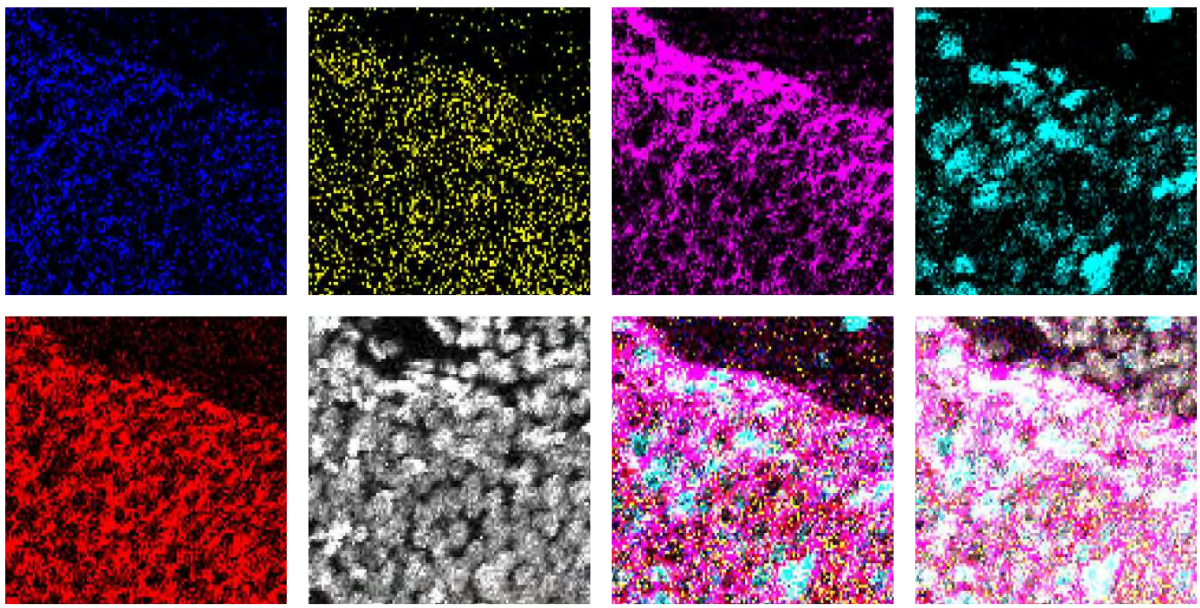

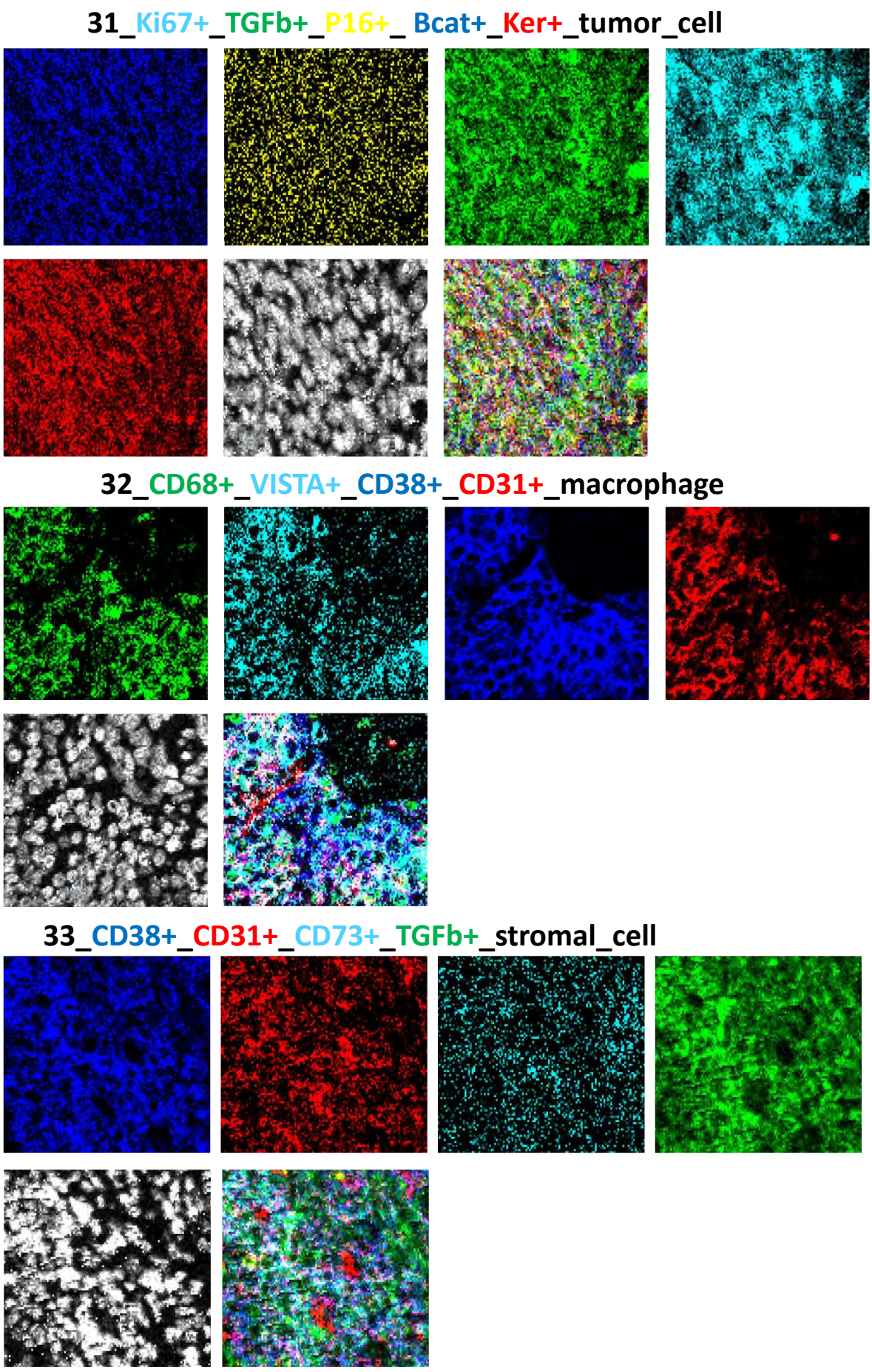
31_Ki67+_TGFb+_P16+_ Bcat+_Ker+_tumor_cell
32_CD68+_VISTA+_CD38+_CD31+_macrophage
33_CD38+_CD31+_CD73+_TGFb+_stromal_cell

34_CD3+_CD4+_CD7+_CD73+_CD38+_TGFb _CD45ro+_T_cell

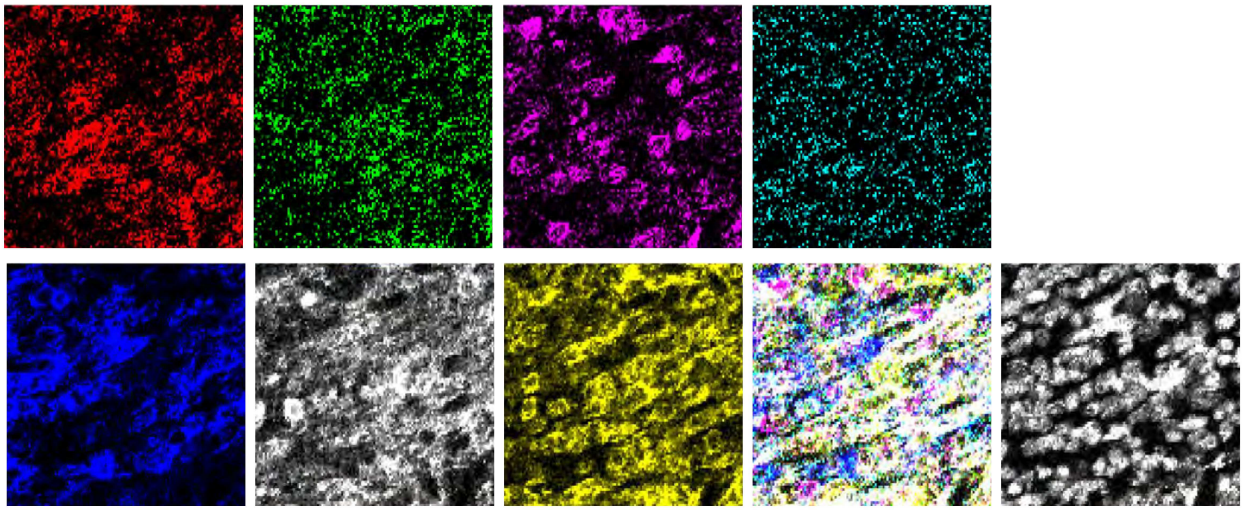

35_CD3+_CD4+_CD7+_CD73+_TGFb+_CD45ro+_T_cell

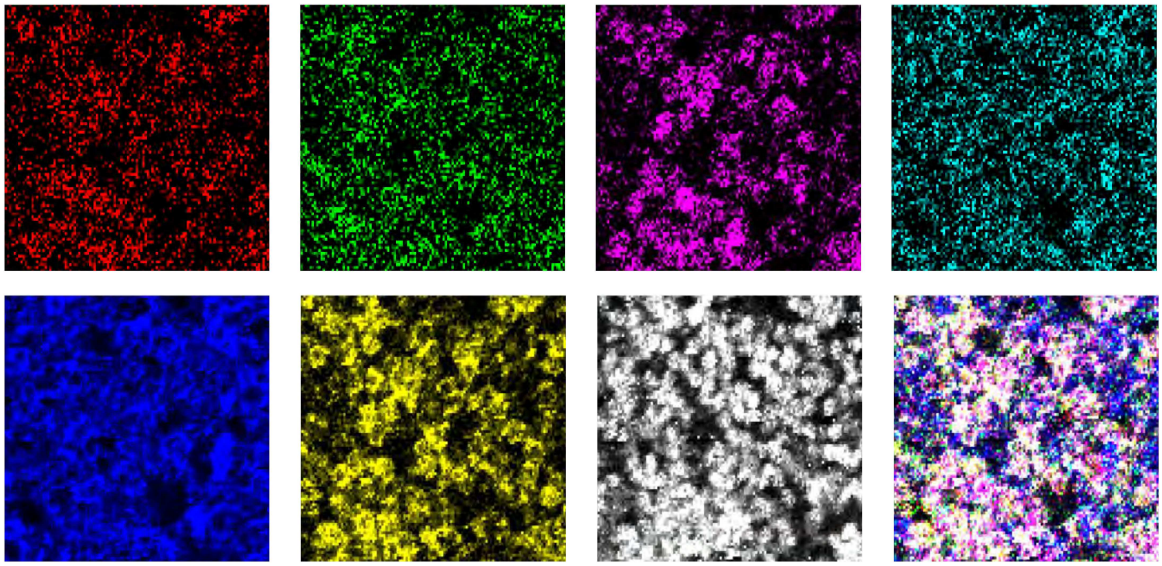

36_CD3+_CD8+_CD7+_TGFb+_CD45ro+_T_cell

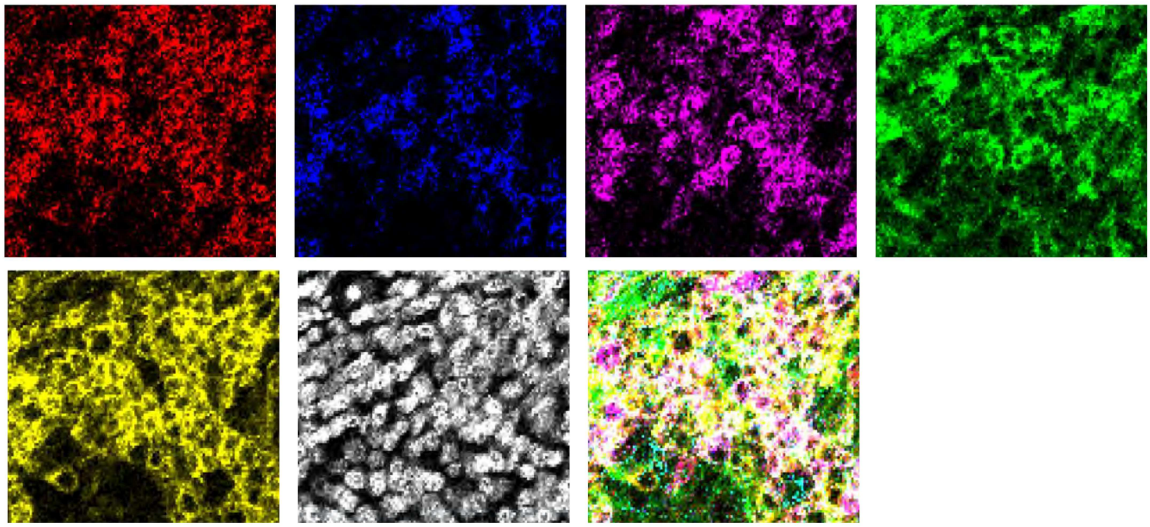

37_CD3+_CD4+_CD7+_ICOS+_CD103+_D240+_CD45ro+_T_cell

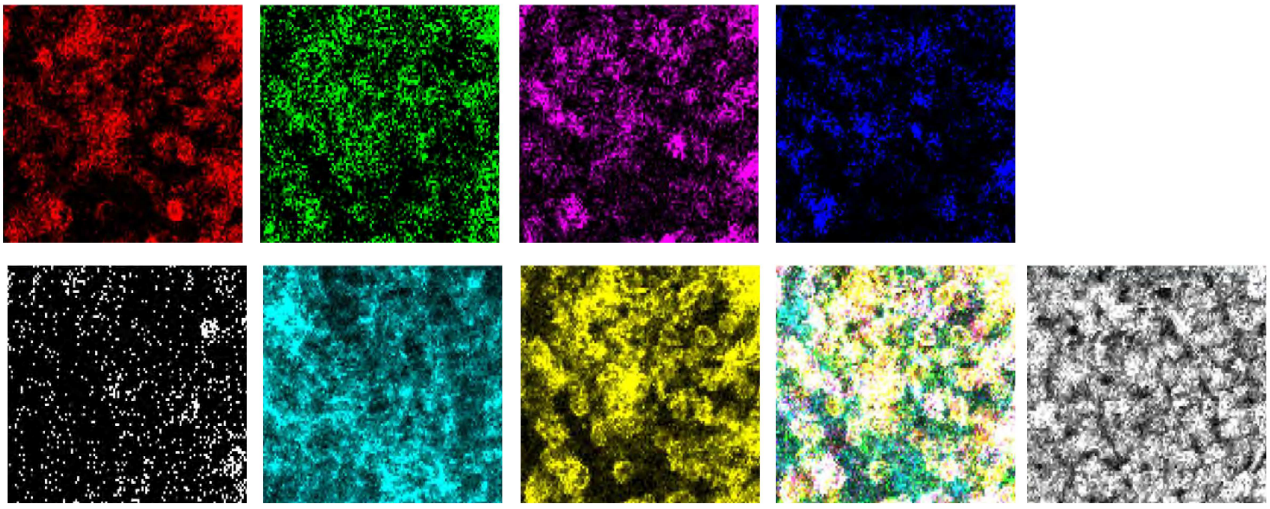

38_CD68+_CD14+_CD204+_CD11c+_HLADR+_macrophage

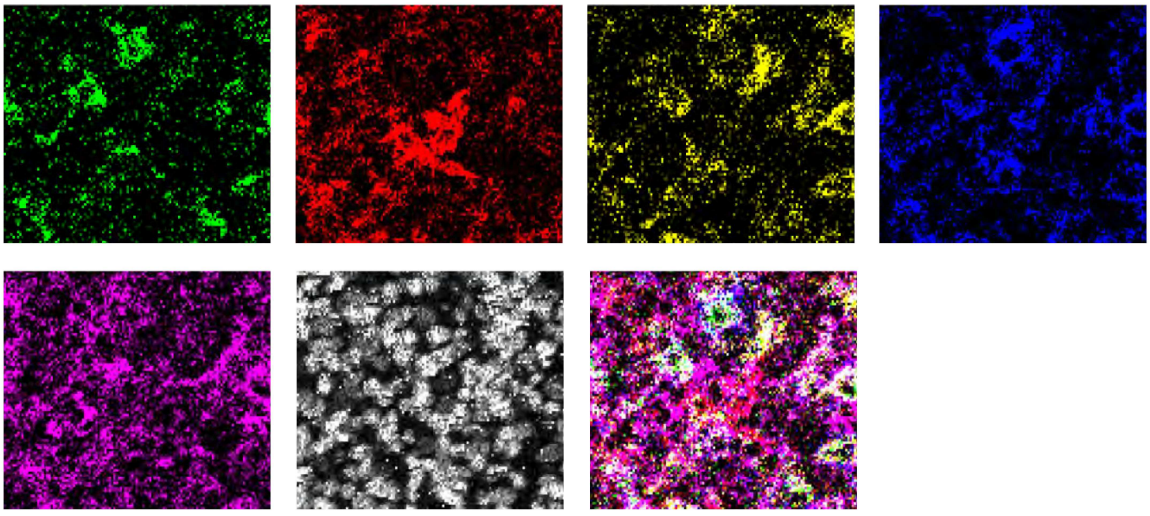

39_CD68+_CD163+_CD14+_CD204+_CD11c+_HLADR+_macrophage

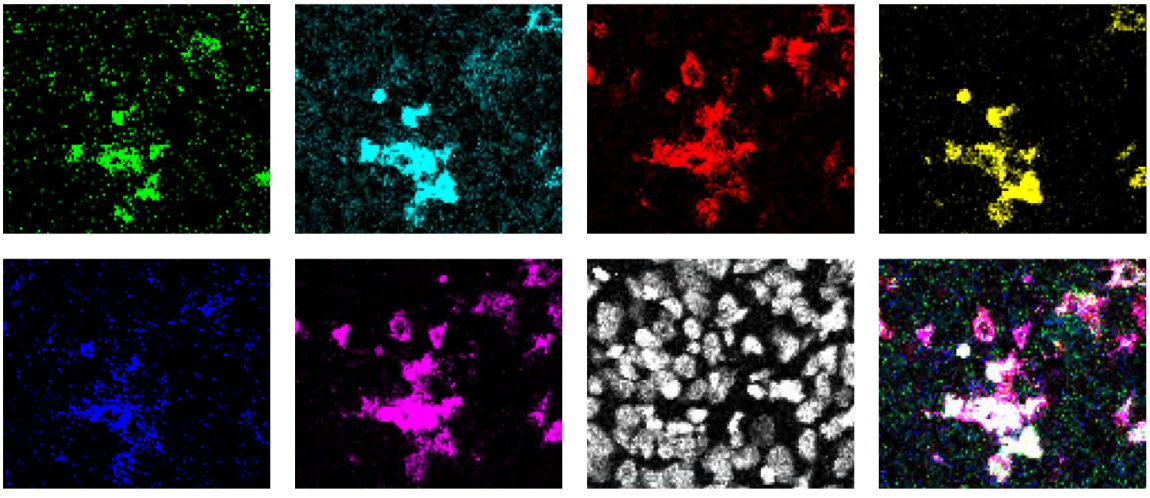

40_VISTA+_CD103+_Bcat+_Ker+_tumor_cell

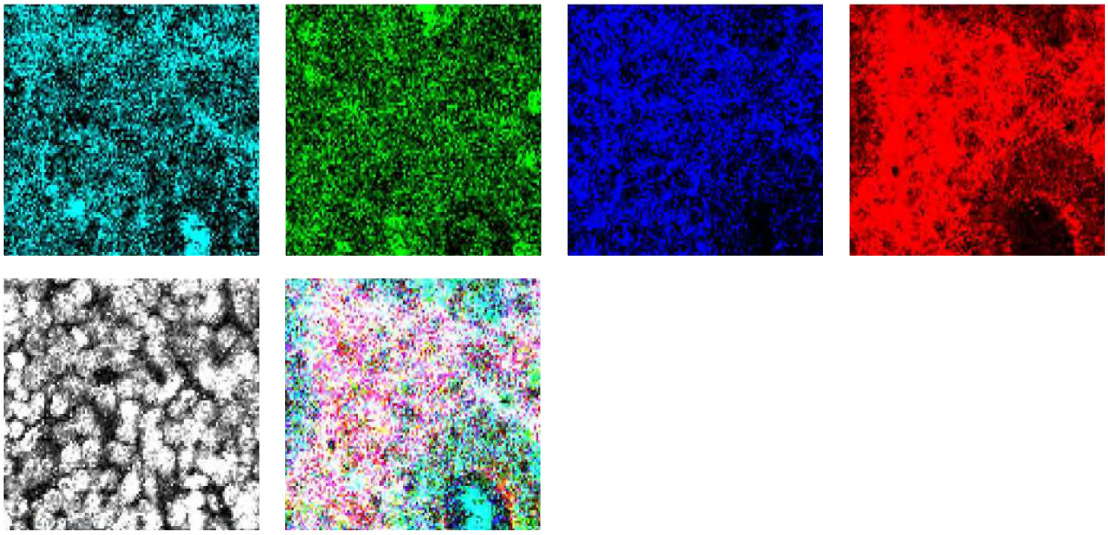

41_CD20+_HLADR+_Ki67+_CD45+_B_cell

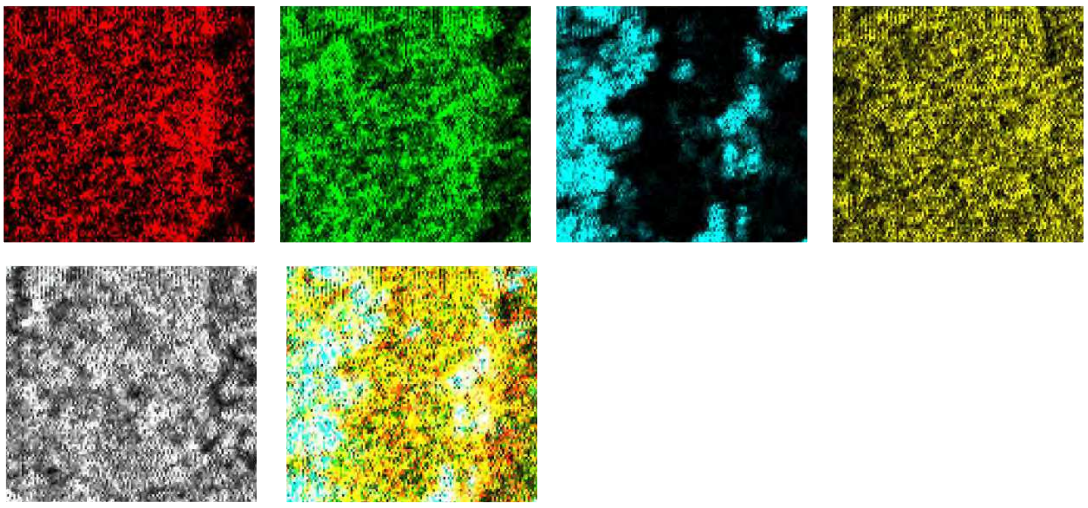

42_CD3+_CD4+_CD7+_FOXP3+_D240+_CD45ro+_Treg

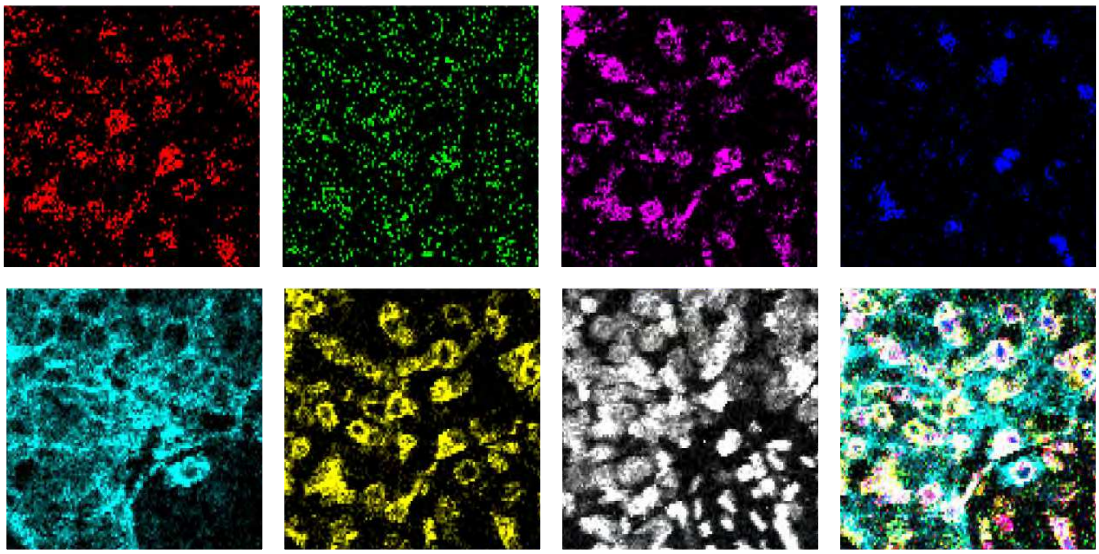

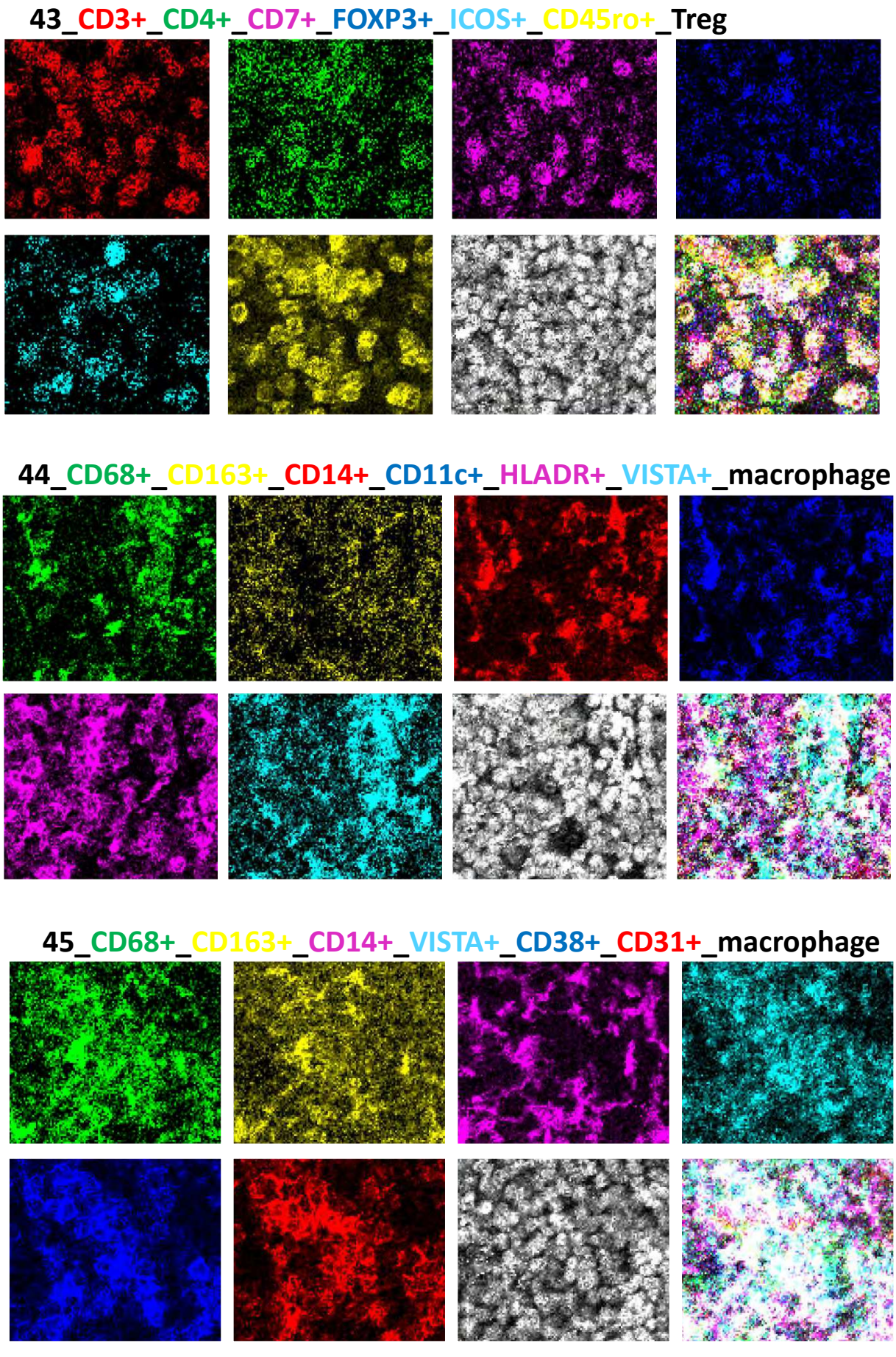
43_CD3+_CD4+_CD7+_FOXP3+_ICOS+_CD45ro+_Treg
44_CD68+_CD163+_CD14+_CD11c+_HLADR+_VISTA+_macrophage
45_CD68+_CD163+_CD14+_VISTA+_CD38+_CD31+_macrophage

46_PDL1+_P16+_Bcat+_Ker+_tumor_cell

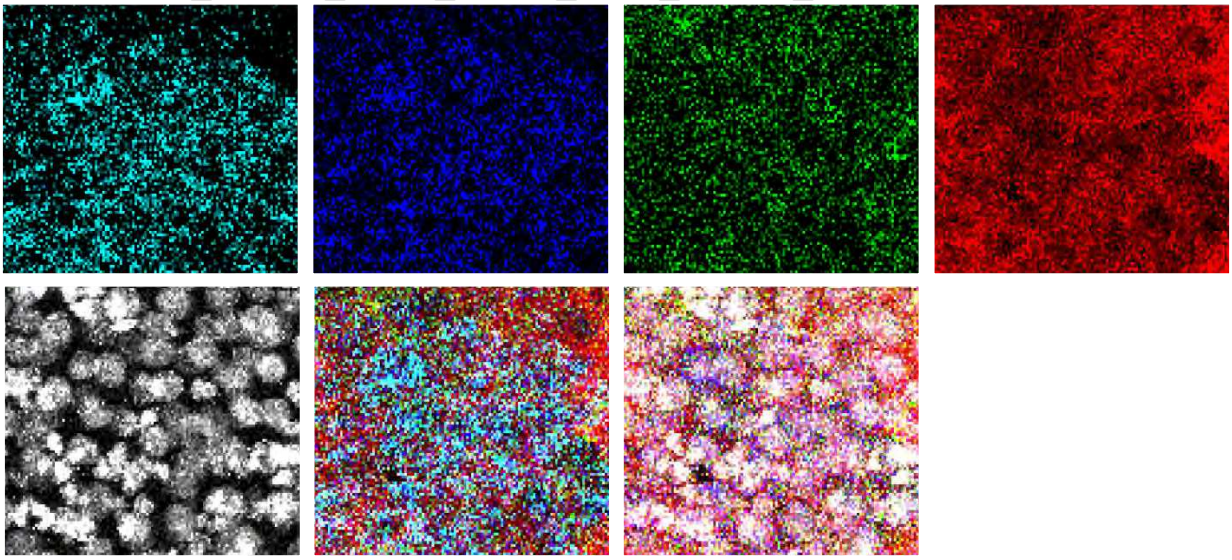

47_IDO+_PDL1+_P16+_Bcat+_Ker+_tumor_cell

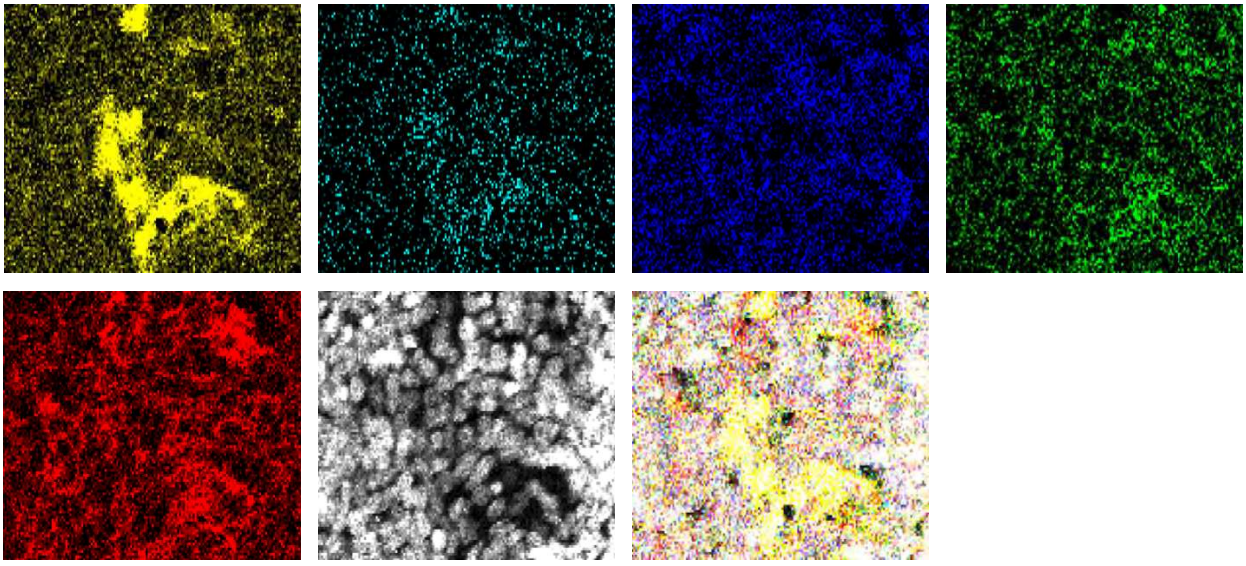

48_CD11b+_CD15+_VISTA+_CD45ro+_granulocyte

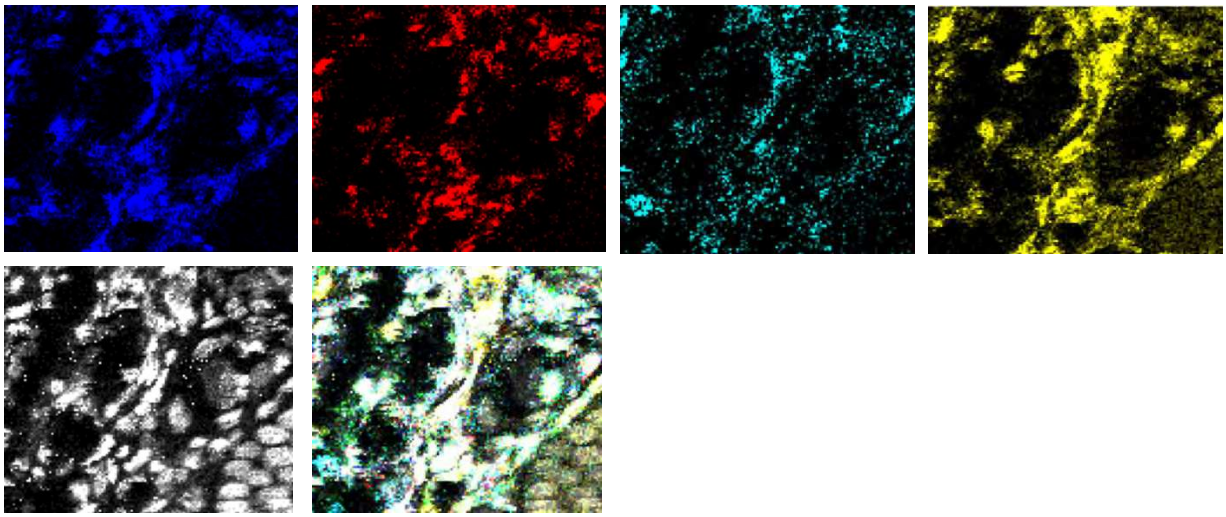

49_CD11b+_CD15+_CD45ro+_granulocyte

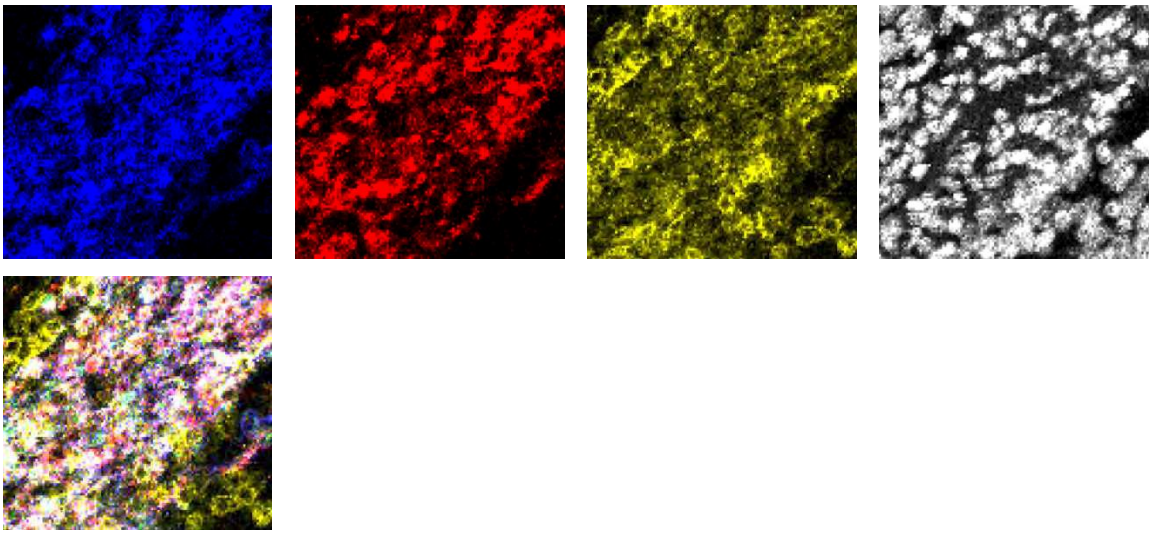

50_Caspase+_Bcat+_Ker+_tumor_cell

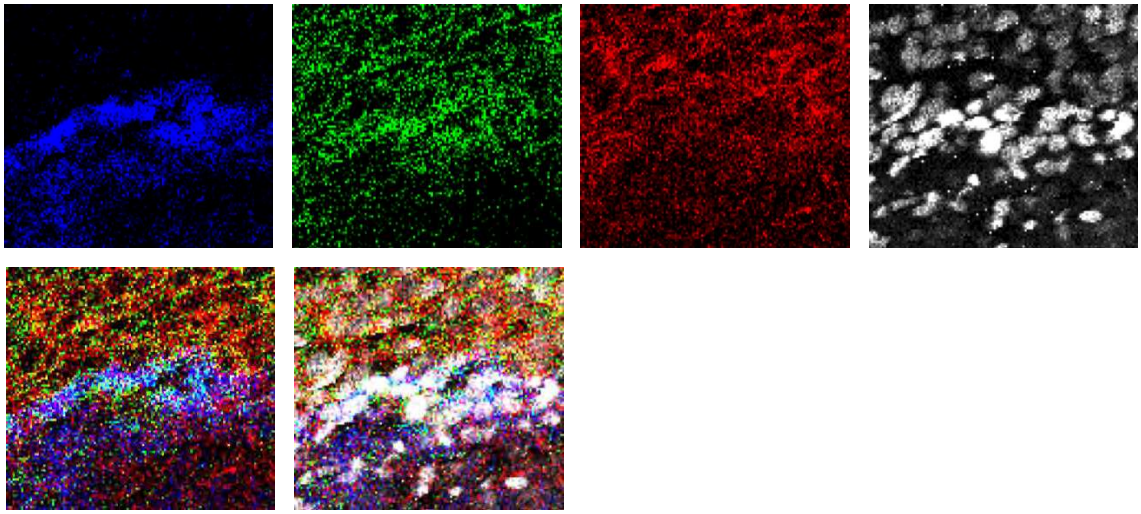

51_CD68+_CD163+_macrophage

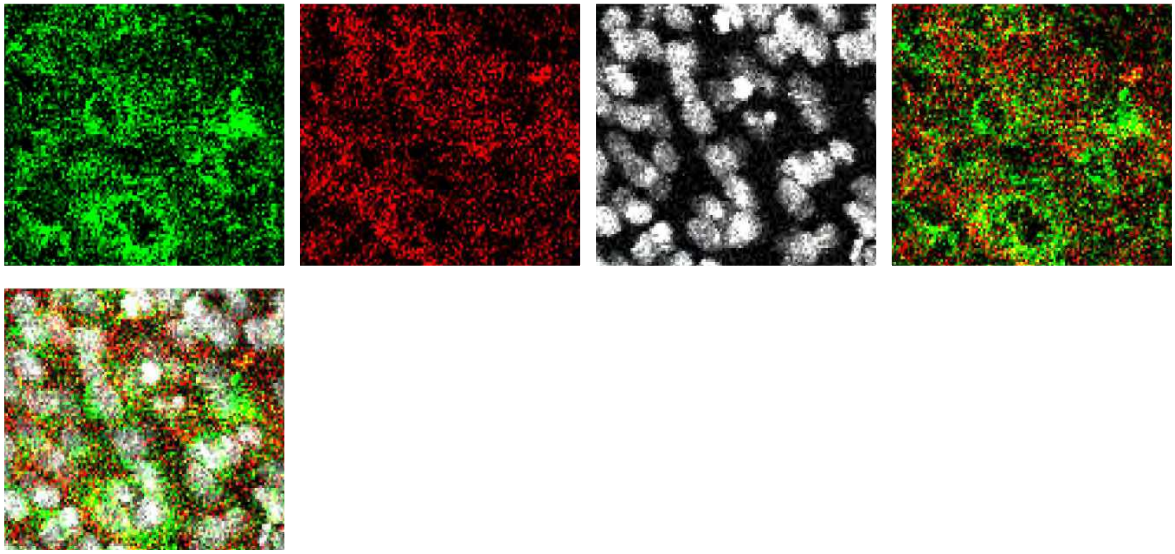

A

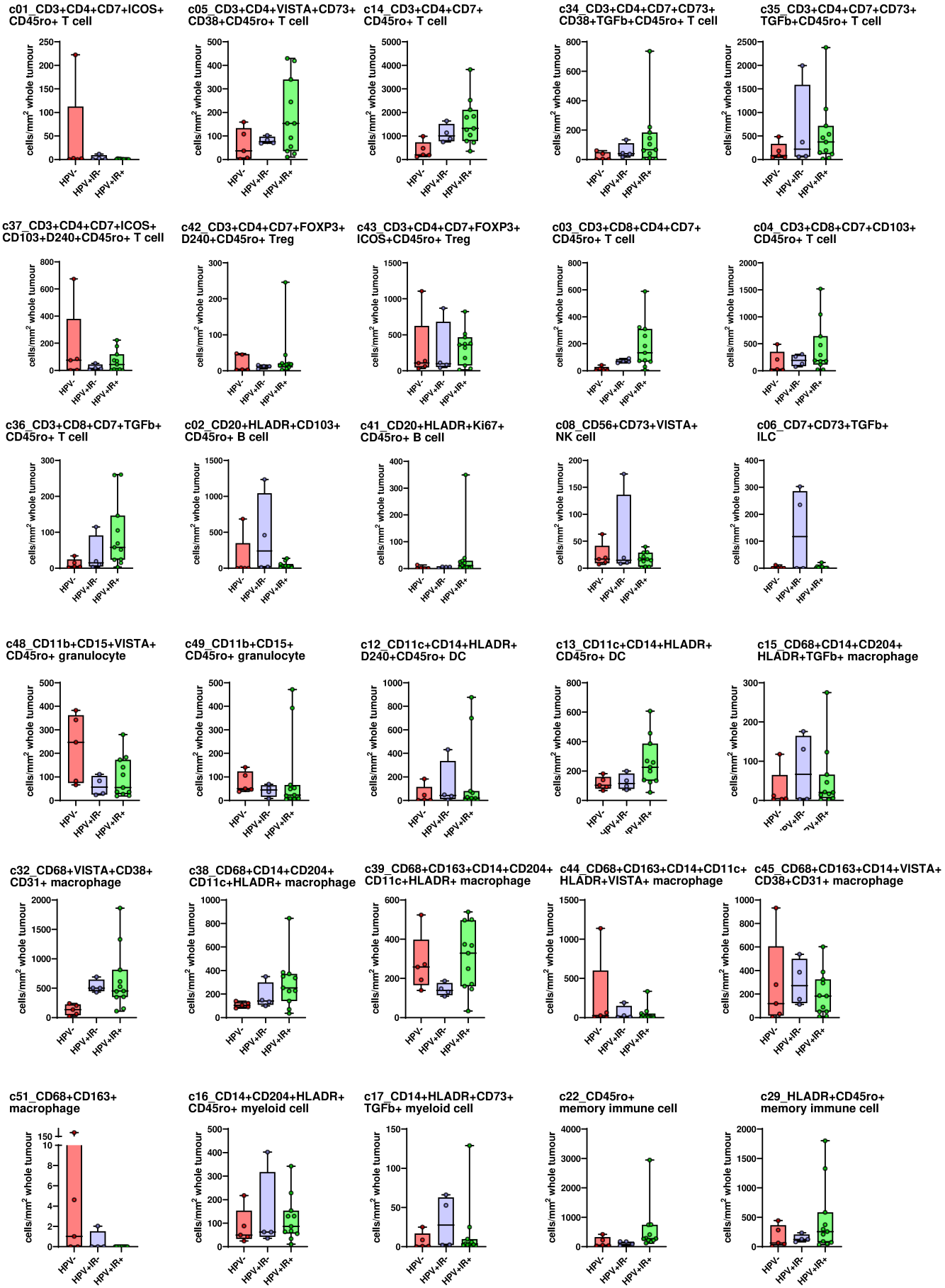
c01_CD3+CD4+CD7+ICOS+ CD45ro+ T cell
c05_CD3+CD4+VISTA+CD73+ CD38+CD45ro+ T cell
c14_CD3+CD4+CD7+ CD45ro+ T cell
c34_CD3+CD4+CD7+CD73+ CD38+TGFb+CD45ro+ T cell
c35_CD3+CD4+CD7+CD73+ TGFb+CD45ro+ T cell
c37_CD3+CD4+CD7+ICOS+ CD103+D240+CD45ro+ T cell
c42_CD3+CD4+CD7+FOXP3+ D240+CD45ro+ Treg
c43_CD3+CD4+CD7+FOXP3+ ICOS+CD45ro+ Treg
c03_CD3+CD8+CD4+CD7+ CD45ro+ T cell
c04_CD3+CD8+CD7+CD103+ CD45ro+ T cell
c36_CD3+CD8+CD7+TGFb+ CD45ro+ T cell
c02_CD20+HLADR+CD103+ CD45ro+ B cell
c41_CD20+HLADR+Ki67+ CD45ro+ B cell
c08_CD56+CD73+VISTA+ NK cell
c06_CD7+CD73+TGFb+ ILC
c48_CD11b+CD15+VISTA+ CD45ro+ granulocyte
c49_CD11b+CD15+ CD45ro+ granulocyte
c12_CD11c+CD14+HLADR+ D240+CD45ro+ DC
c13_CD11c+CD14+HLADR+ CD45ro+ DC
c15_CD68+CD14+CD204+ HLADR+TGFb+ macrophage
c32_CD68+VISTA+CD38+ CD31+ macrophage
c38_CD68+CD14+CD204+ CD11c+HLADR+ macrophage
c39_CD68+CD163+CD14+CD204+ CD11c+HLADR+ macrophage
c44_CD68+CD163+CD14+CD11c+ HLADR+VISTA+ macrophage
c45_CD68+CD163+CD14+VISTA+ CD38+CD31+ macrophage
c51_CD68+CD163+ macrophage
c16_CD14+CD204+HLADR+ CD45ro+ myeloid cell
c17_CD14+HLADR+CD73+ TGFb+ myeloid cell
c22_CD45ro+ memory immune cell
c29_HLADR+CD45ro+ memory immune cell
cells/mm2 whole tumour
HPV-
HPV+IR-
HPV+IR+

B

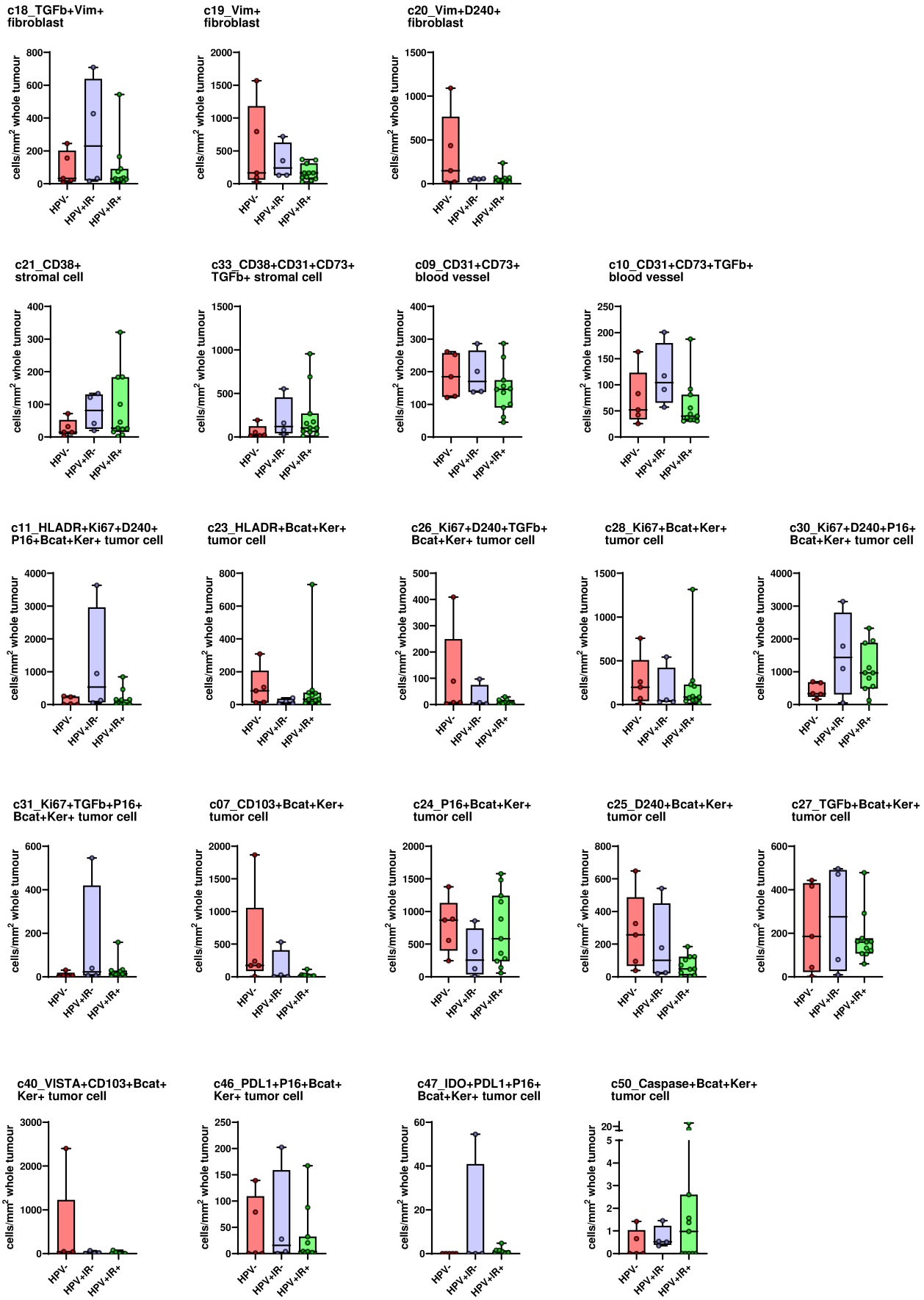

Supplemental Figure 5. Imaging mass cytometry quantitative findings 51 clusters.
Boxplots showing quantitative comparisons of all 51 identified different cell clusters present in the whole tumor. In **A)** the immune cell clusters and in **B)** the other cell clusters. The three distinct OPSCC subgroups are indicated by different dot colors: HPV^- red (n=5), $HPV16^+IR^-$ blue (n=4) and $HPV16^+IR^+$ green (n=11). Boxplots with bars in box representing the median and interquartile range

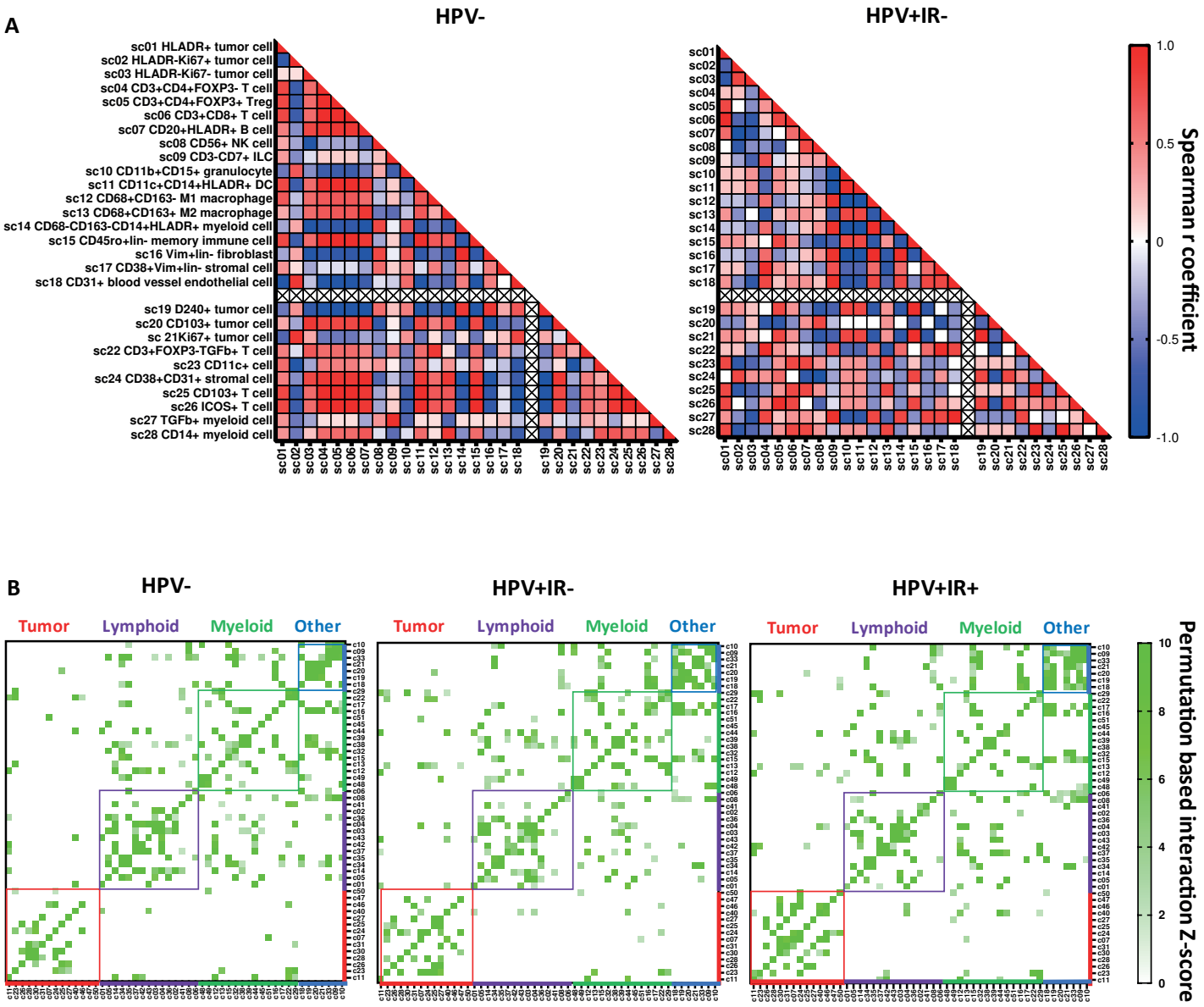

Supplemental Figure 6. Permutation testing of spatial cellular interactions.
A) Spearman quantitative correlation heatmaps of the 28 superclusters (18 mutually exclusive, and 10 non-mutually exclusive) in the whole tumor for HPV- (n=5) and HPV16+IR- (n=4) OPSCC. **B)** Heatmap of permutation based Z-scores for spatial interactions between the 51 identified clusters, in HPV- (n=5), HPV16+IR- (n=4) and HPV16+IR+ (n=11) OPSCC. Only interactions with a permutation based Z-score>2 (i.e. outside the 95% normal distribution range) are visualized.

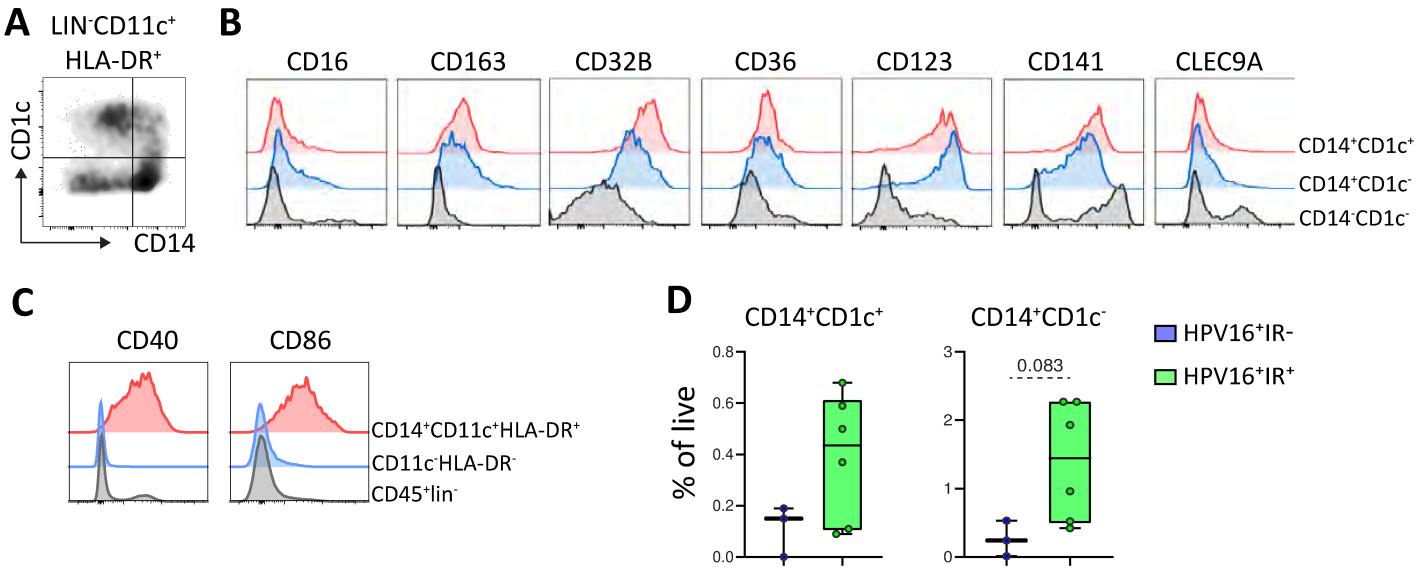

Supplemental Figure 7. Characterization of CD14⁺CD1c⁺ DC and CD14⁺CD1c- monocytes/macrophages in the TME of HPV16⁺IR- and HPV16⁺IR⁺ OPSCC tumors.

Freshly dissociated OPSCC tumor tissue from 9 HPV16⁺ OPSCC patients was analyzed by 13-parameter flow cytometry analysis with antibodies directed against CD3/CD19/CD20/CD56, CD11c, HLA-DR, CD14, CD11b, CD163, CD141, CLEC9A, CD1c, CD16, CD123, CD36 and CD32B. **A, B)** The gating strategy is depicted for a representative OPSCC sample. **A)** Dot plot showing expression of CD14 and CD1c within lineage-negative (LIN-), CD11c⁺ and HLA-DR⁺ myeloid cells. Singlets were gated on FSC-H/FSC-A properties, after which dead cells were excluded through gating on yellow amine reactive dye-negative cells. Next, CD3-CD19-CD20-CD56-HLA-DR⁺CD11c⁺ myeloid cells were selected, which were subsequently divided based on CD14 and CD1c expression. **B)** Histogram plots showing CD16, CD163, CD32B, CD36, CD123, CD141 and CLEC9A expression for CD14-CD1c- (black), CD14⁺CD1c- (blue) and CD14⁺CD1c⁺ cells (red). **C)** Histogram plots showing CD40 and CD86 expression for CD45⁺lin- (black), CD11c-HLA-DR- (blue) and CD14⁺CD11c⁺HLA-DR⁺ cells (red). **D)** Box plots depicting the distribution of the identified CD14⁺CD1c⁺ DC (left) and CD14⁺CD1c- monocytes/macrophages (right) among HPV16⁺IR- (blue, n=3) and HPV16⁺IR⁺ (green, n=6) OPSCC tumors. Data is represented as percentage of live cells.

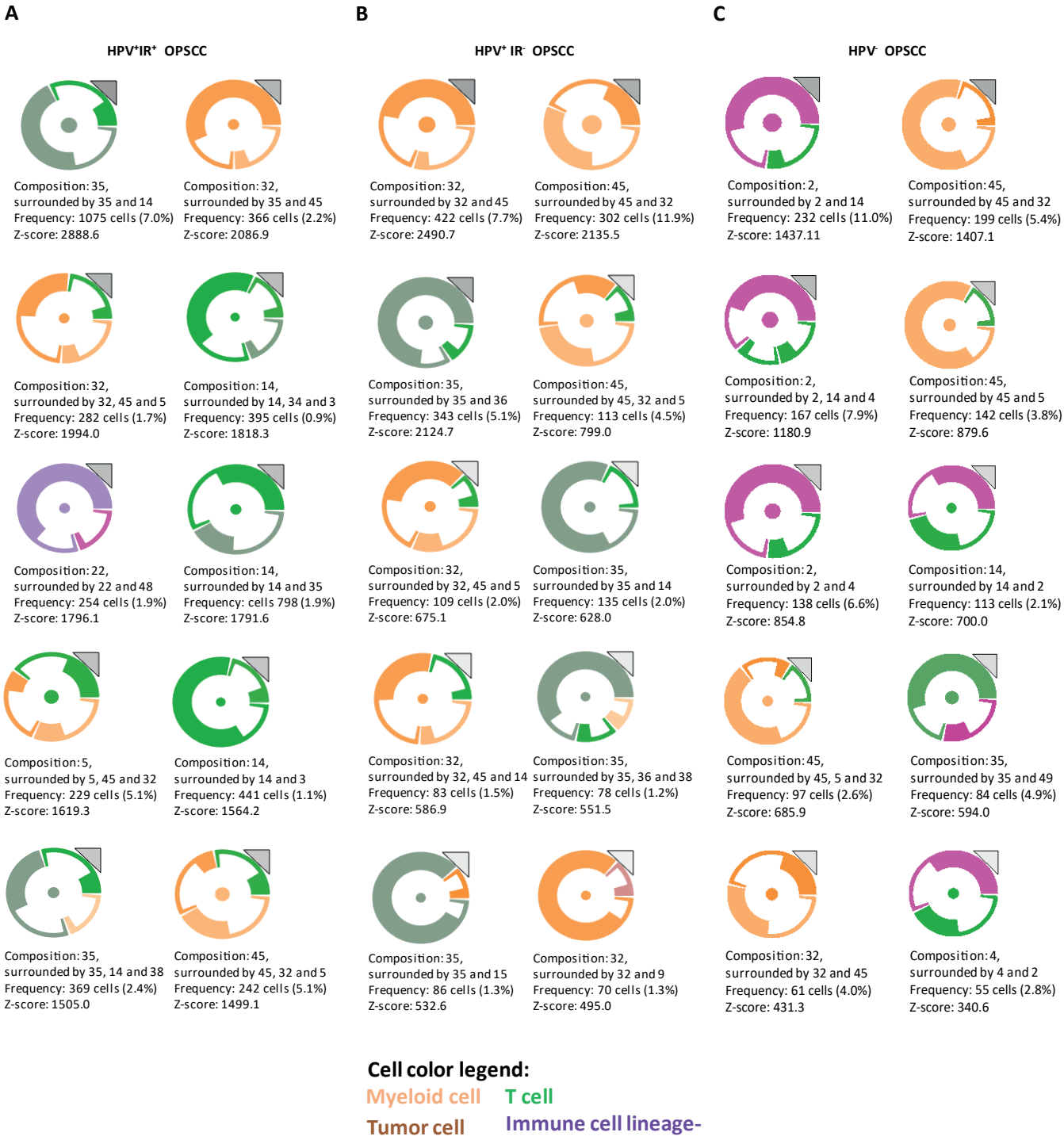

Supplemental Figure 8. Top 10 360° spatial immune compositions per OPSCC subgroup.
Top 10 360° spatial immune compositions with the highest Z-scores are depicted. In **A)** HPV16+IR+ (n=11), **B)** HPV16+IR- (n=4), and **C)** HPV- (n=5) OPSCC. Clusters, frequency and Z-score are described below each composition. Interaction neighborhood is defined as 5µm (direct spatial cellular interaction). Threshold for the 360° compositions: ≥20 occurrences.

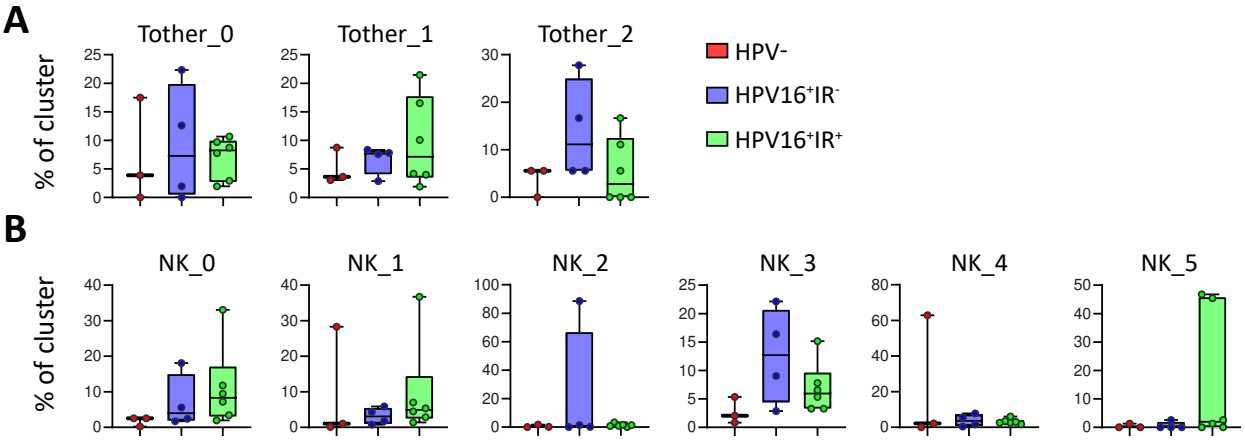

Supplemental Figure 9. Distribution of the identified clusters among HPV-, HPV16+IR- and HPV16+IR+ OPSCC tumors.

Magnetic-bead sorted CD3+ T cells and CD56+ NK cells from 13 OPSCC samples were analyzed by integrated single-cell transcriptome and TCR repertoire RNA sequencing analysis. Box plots depict the distribution of the Tother **(A)** and NK **(B)** cell clusters among HPV- (red, n=3), HPV16+IR- (blue, n=4) and HPV16+IR+ (green, n=6) OPSCC tumors. Data is represented as percentage of cluster. * p-value<0.05.

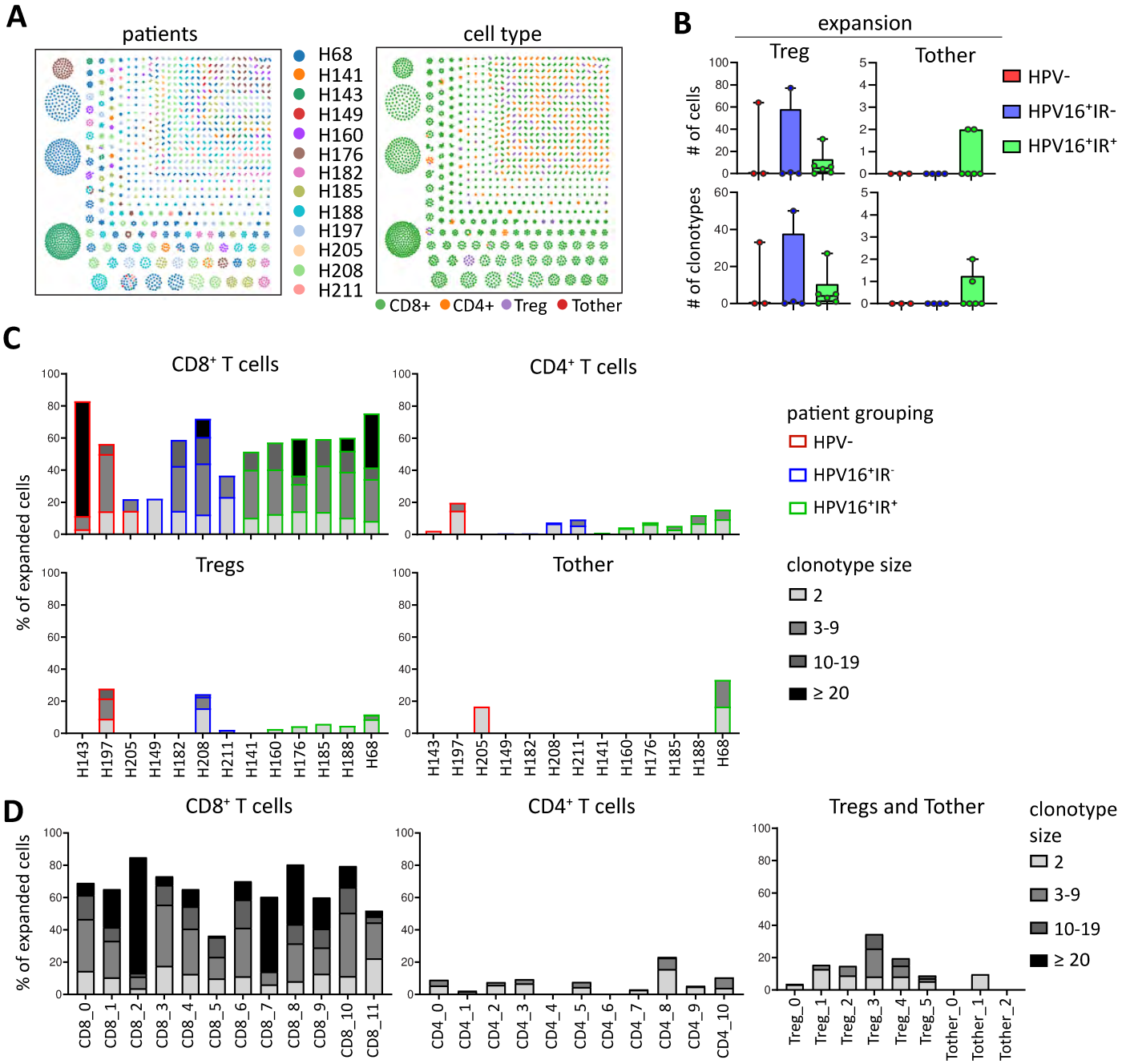

Supplemental Figure 10. Clonotype size among individual OPSCC and T cell clusters. Magnetic-bead sorted CD3+ T cells and CD56+ NK cells from 13 OPSCC samples were analyzed by integrated single-cell transcriptome and TCR repertoire RNA sequencing analysis. A) Graphs depicting the expanded clonotype clusters, colored by patient (left) and cell type (right). B) Box plots displaying the number of expanded cells (top) and clonotypes (bottom) within Tregs (left) and Tother (right) cells detected in HPV- (red, n=3), HPV16+IR- (blue, n=4) and HPV16+IR+ (green, n=6) OPSCC patients. C, D) Graphs depicting the clonotype size of the expanded TCR in CD8+ T cells, CD4+ T cells, Treg and Tother cells per patient (C) and per cluster (D). Data is given as percentage of expanded CD8, CD4, Treg or Tother cells. Colored outline indicates the HPV- and immune response status (HPV- (red, n=3), HPV16+IR- (blue, n=4) and

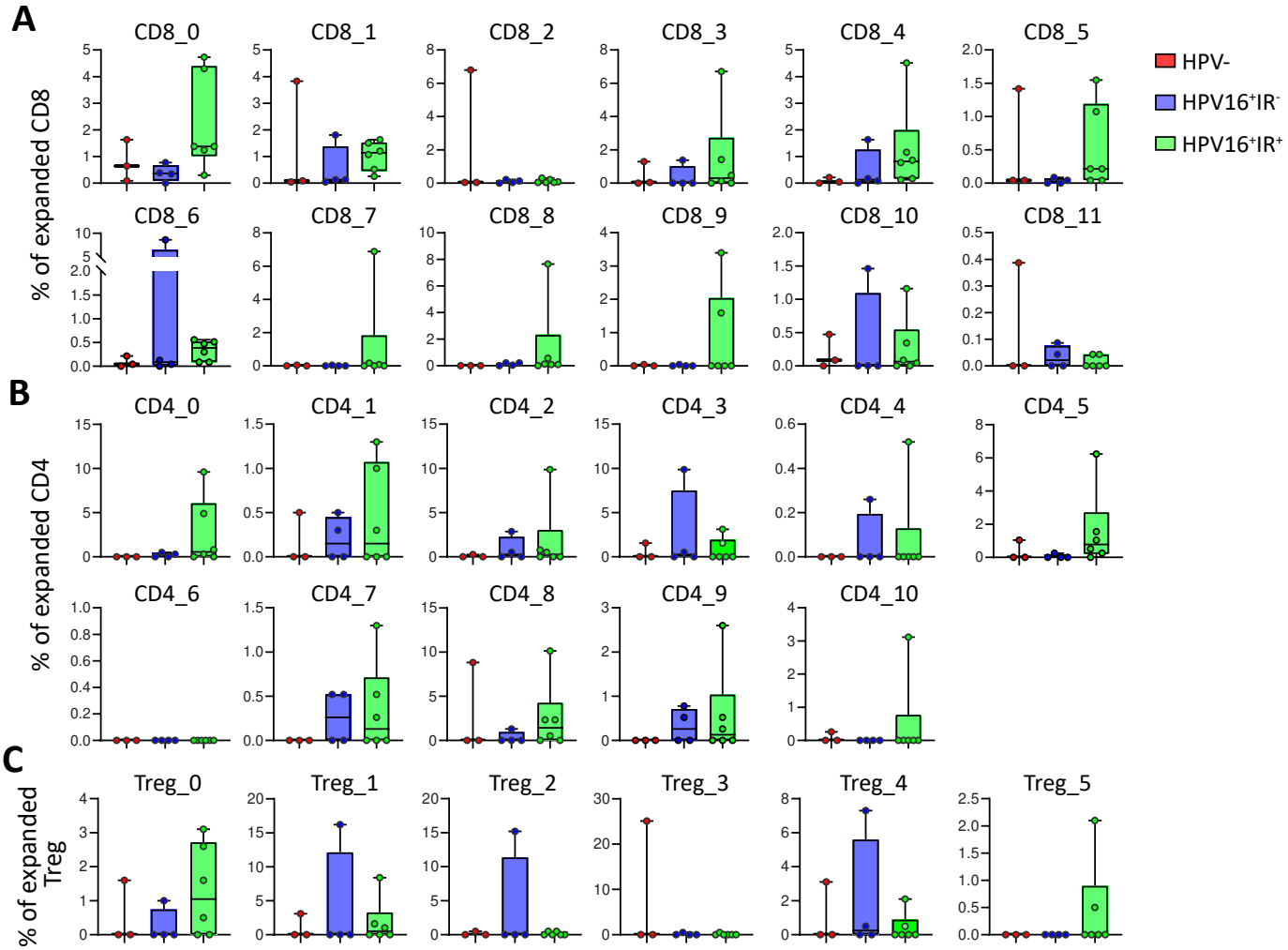

Supplemental Figure 11. T cell expansion among the different T cell clusters.
Integrated single-cell transcriptome and TCR repertoire RNA sequencing analysis was performed on magnetic-bead sorted CD3+ T cells and CD56+ NK cells from 13 OPSCC samples. A-C) Box plots displaying the percentage of expanded cells within the identified CD8 **(A)**, CD4 **(B)** and Treg **(C)** clusters in HPV- (red, n=3), HPV16+IR- (blue, n=4) and HPV16+IR+ (green, n=6) OPSCC patients. Data are represented as percentage of total expanded CD8, CD4 and Treg cells.

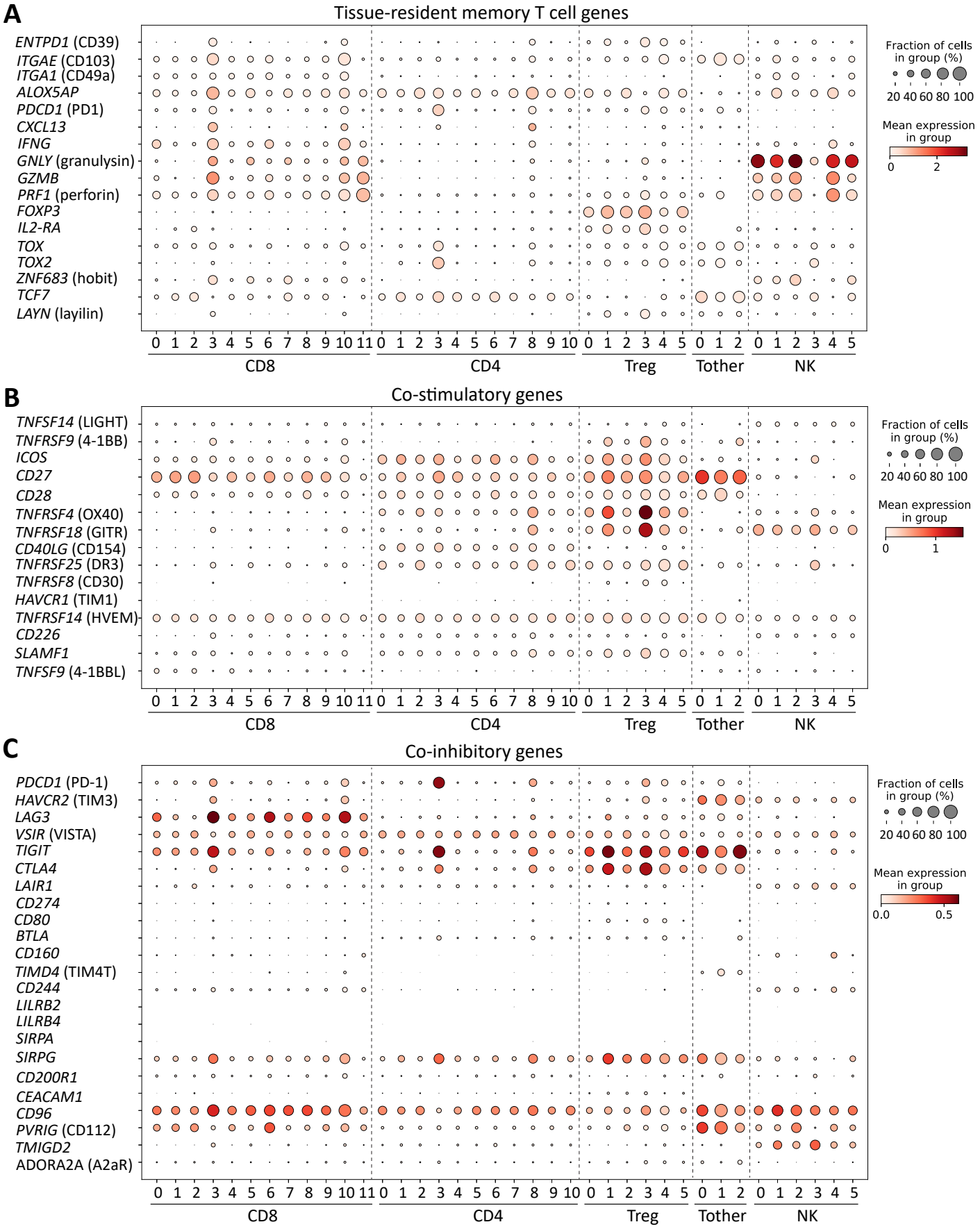

Supplementary Figure 12. Expression of tissue-resident memory T cell, co-stimulatory and co-inhibitory markers within the intratumoral CD8, CD4, Treg, Tother and NK cell cluster in OPSCC.

Single-cell transcriptome RNA sequencing analysis was performed on magnetic-bead sorted $CD3^+$ T cells and $CD56^+$ NK cells from 13 OPSCC samples. Dot plots depict the expression levels of **A**) tissue-resident memory T cell, **B**) co-stimulatory and **C**) co-inhibitory genes (Y-axis) for all identified CD8, CD4, Treg, Tother and NK clusters (X-axis, from left to right). The size of the dots represent the percentage of cells expressing the genes, and the color scale indicates the mean expression of the genes.

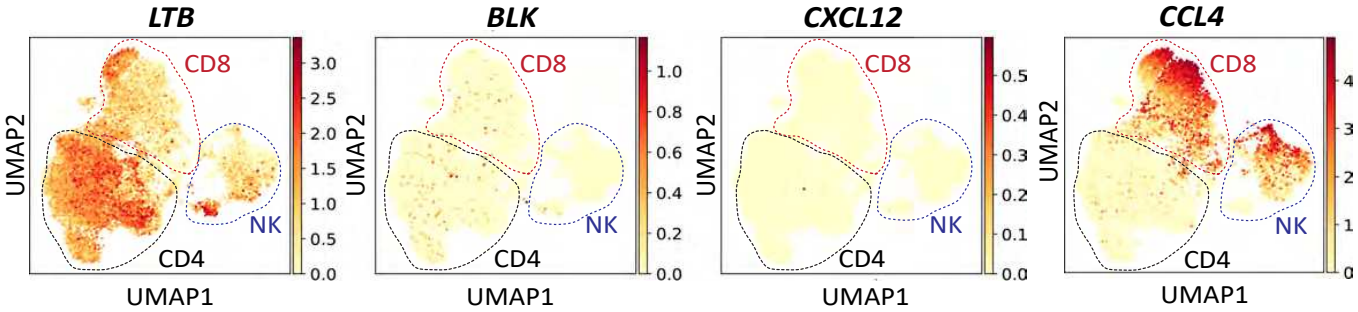

Supplemental Figure 13. Expression of LTB, BLK, CXCL12, CCL4, XCL1 and LMNA within T cells and NK cells. Two-dimensional UMAP plots displaying single cell transciptomics of 14,242 T cells and 2,820 NK cells from 13 OPSCC patients. Each dot represents a single cell. Expression levels of LTB, BLK, CXCL12 and CCL4 are depicted in color code. Dotted borders denote where CD4, CD8 and NK cell clusters are located.

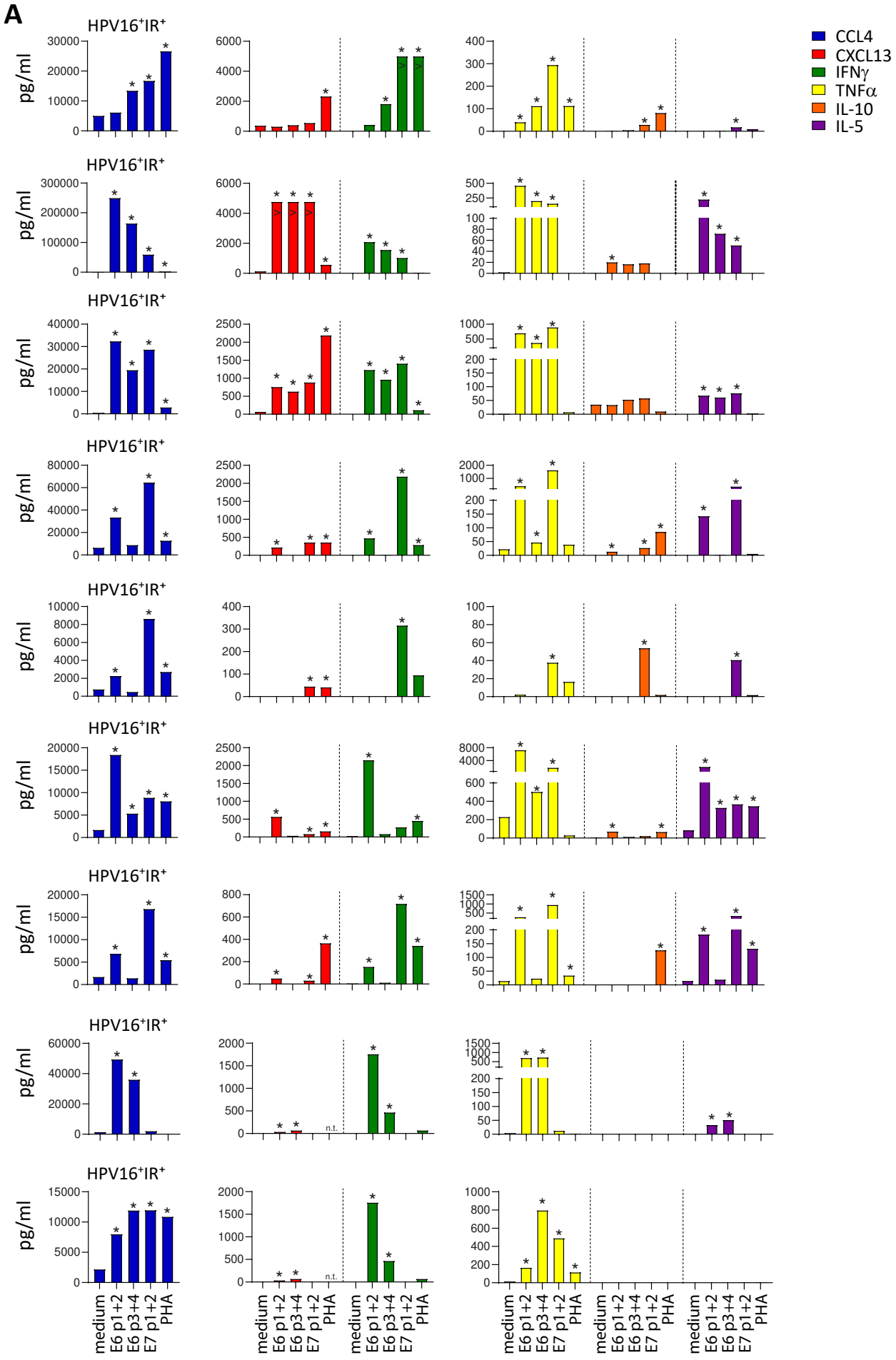
A
HPV16+IR+
pg/ml
CCL4
CXCL13
IFNγ
TNFα
IL-10
IL-5
n.t.
medium
E6 p1+2
E6 p3+4
E7 p1+2
PHA

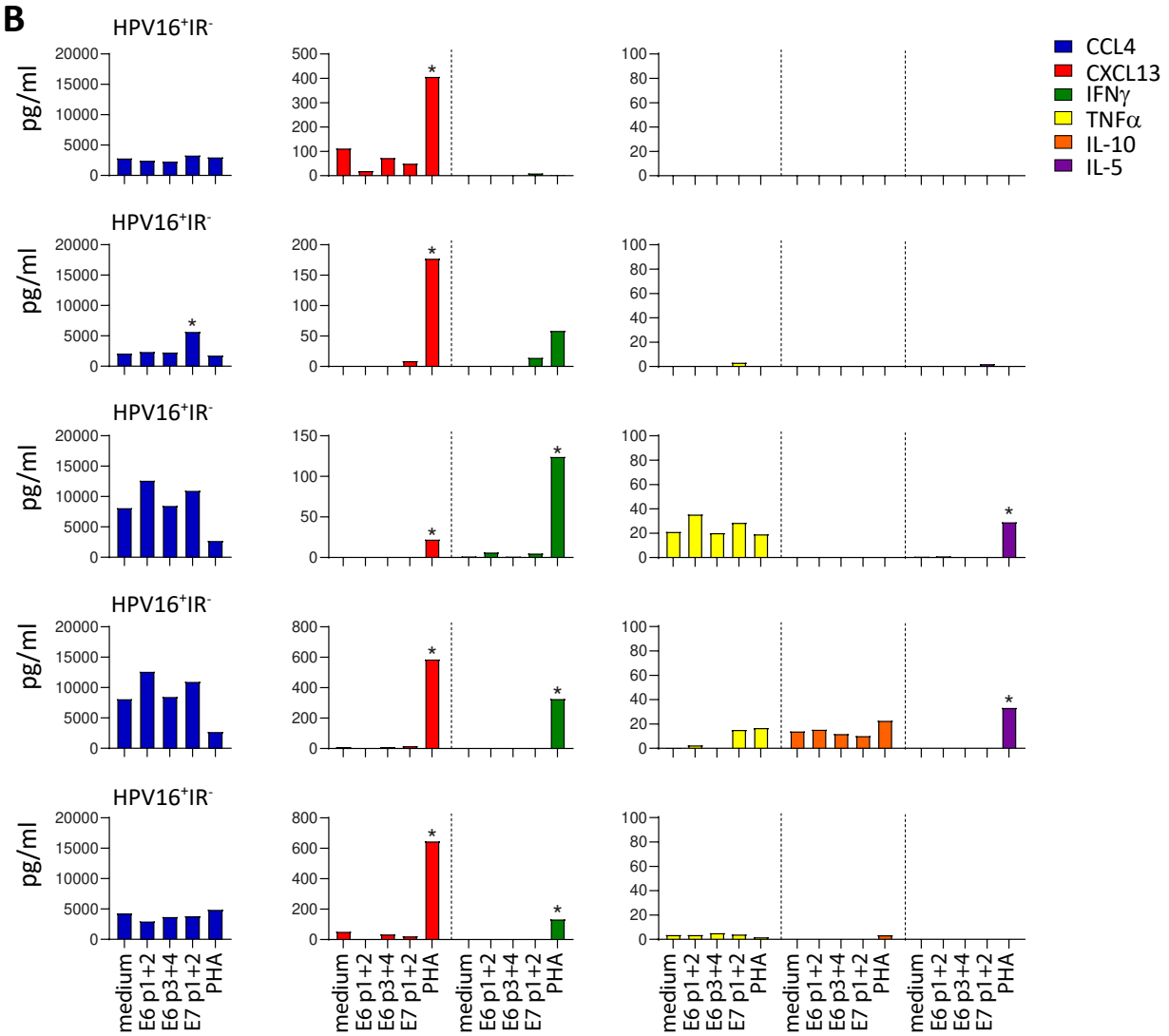

Supplemental Figure 14. HPV reactivity of cultured OPSCC TIL. Graphs displaying CCL4 (blue), CXCL13 (red), IFNγ (green), TNFα (yellow), IL-10 (orange) and IL-5 (purple) production of cultured OPSCC TIL in response to medium, HPV16 E6 peptide (pool 1+2 and 3+4), HPV16 E7 peptide (pool 1+2)-loaded autologous monocytes for HPV16^{+}IR^{+} (n=9; **A**) and HPV16^{+}IR^{-} (n=5; **B**) OPSCC. Cytokine production in response to PHA served as positive control. Positive cytokine production, which is defined as at least twice above that of the cells stimulated with medium-loaded monocytes, is indicated by the asterisk. CCL4 and CXCL13 were determined by a multiplex cytokine assay and IFNγ, TNFα, IL-10 and IL-5 by cytometric bead array.

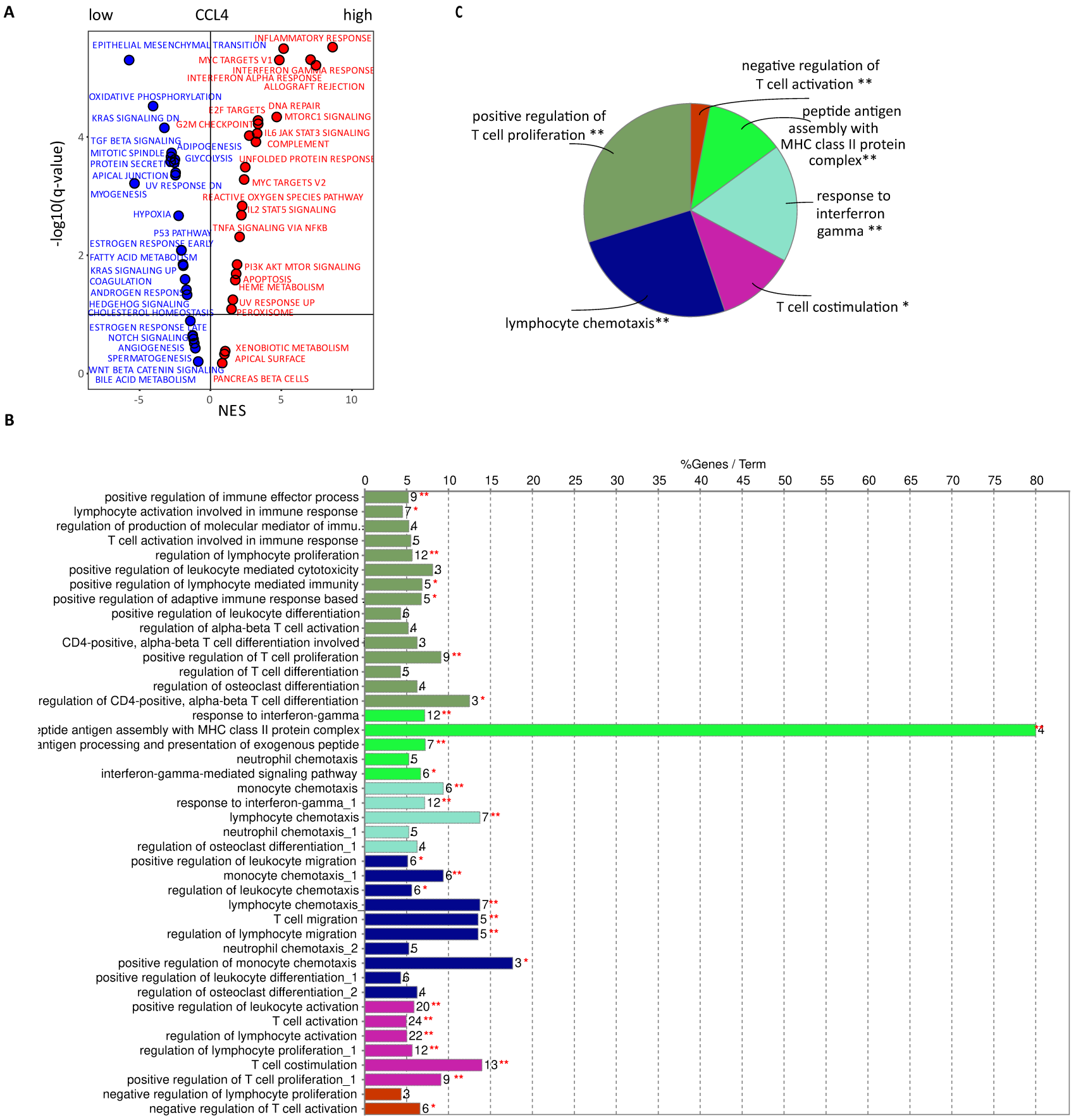

Supplemental Figure 15. CCL4 expression is associated with a productive tumor immune microenvironment. **A)** High expression of CCL4 is positively associated with the hallmark gene sets of tumor rejection and negatively associated with the hallmarks of tumor promotion. The log2 fold change level of each gene between a high and low group was used as input for the GSEA-preranked. The GSEA was performed using the Molecular Signatures Database (MSigDB). The 50 hallmark gene sets were illustrated by their normalized enrichment score (NES). Red and blue dots show the enrichment and depletion of hallmark gene sets, respectively. **B)** ClueGO analysis of highly significant associated genes with high expression of CCL4 in the tumor microenvironment (R>0.7 and R>0.4, respectively, adj-value <0.05). The bars represent the percentage of highly significantly correlated genes associated with the GO terms (%Genes/term). The number of expressed genes per term is shown as bar label. P-value is indicated by asterisks. **C)** Overview chart with functional groups including specific terms for highly significantly associated genes with high expression of CCL4. * mid-P values of two-sided (enrichment/depletion) tests based on the hyper geometric distribution (Rivals, 2007, PMID. 17182697).

Tumor specific T cells support chemokine-driven spatial organization of intratumoral immune microaggregates needed for long survival

Ziena Abdulrahman, Saskia J. Santegoets, Gregor Sturm, Pornpimol Charoentong, Marieke E. Ijsselsteijn, Antonios Somarakis, Thomas Höllt, Francesca Finotello, Zlatko Trajanoski, Sylvia L. van Egmond, Dana A.M. Mustafa, Marij J.P. Welters[#], Noel F.C.C. de Miranda[#], Sjoerd H. van der Burg

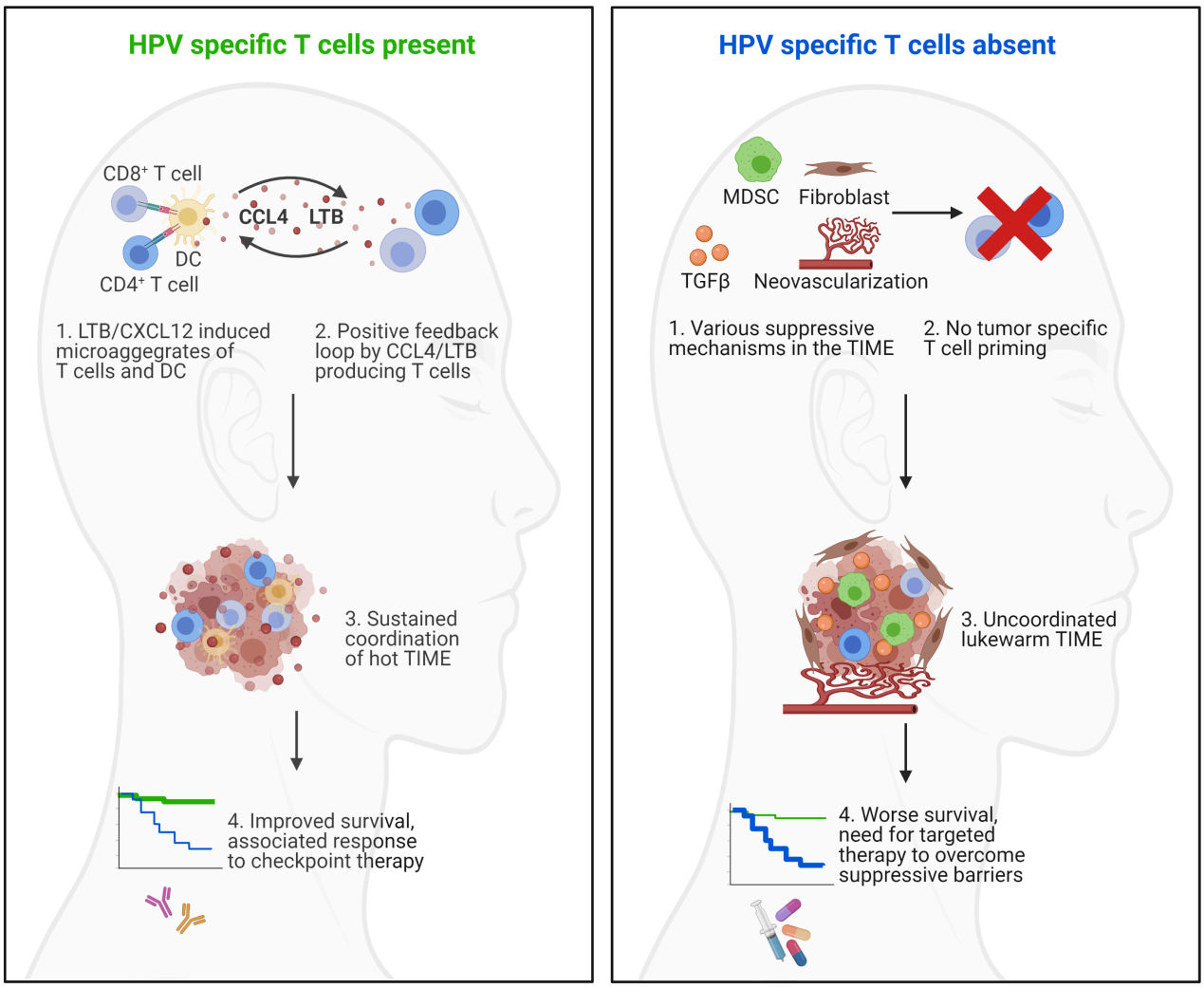

Key findings:

- A specific spatial phenotypic signature (SPS) portrays long surviving oropharyngeal cancer patients
- The SPS consists of intratumoral T cell and dendritic cell microaggregates
- Chemokines produced by tumor-specific T cells sustain the orchestration of the SPS
- Patients lacking this SPS express multiple targetable immunosuppressive mechanisms